Applied Energy 389 (2025) 125785

Contents lists available at ScienceDirect

Applied Energy

journal homepage: www.elsevier.com/locate/apenergy

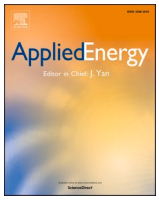

Modelling and analysis of V-shaped bifacial PV systems for agrivoltaic applications: A Python-based approach for energy optimization

Stefania Guarino [a,*], Alessandro Buscemi [a], Christian Chiaruzzi [b], Valerio Lo Brano [a]

[a] Department of Engineering, University of Palermo, Italy
[b] Horizonfirm srl, viale Francesco Scaduto 2/D, Palermo 90143, Italy

HIGHLIGHTS

- A new V-shaped configuration with bifacial modules and single-axis tracking was examined.
- A custom Python algorithm models bifacial energy performance and dynamic tilt.
- The V-shaped bifacial PV configuration generates 2089.3 kWh/year in Palermo's climate.
- V-shaped system reduces land use by 24 % compared to conventional configurations.
- V-shaped PV and conventional setups show no significant differences in energy production.

ARTICLE INFO

Keywords:
Agrivoltaic systems
Bifacial photovoltaic modules
Single-axis tracking system
Land-use optimisation
Energy analysis
Python
PVlib
Solar tracking algorithm
V-shaped

ABSTRACT

Agrivoltaic systems integrate photovoltaic (PV) energy production with agricultural activities, addressing the critical challenges of land use optimization and sustainable energy generation in the context of climate changes and food security. These systems are pivotal in offering a promising solution in mitigating the environmental and social impacts of utility-scale PV installations, such as habitat disruption and competition with agricultural land. This study evaluates a patented V-shaped bifacial photovoltaic system with a single-axis solar tracking, designed to optimize energy capture but also to minimize shading effects on crops like vineyards. A custom Python-based algorithm using PVlib was developed to simulate the performance of the system, accounting for mutual shading, multiple solar radiation reflections, and dynamic tilt adjustments. Simulations conducted for Palermo, Italy, revealed that the system collects 5.2 % less solar irradiation than traditional side-by-side configurations but achieves an annual energy output of 2089.3 kWh per pair of panels, along with 24 % reduction in land use. These results highlight the system capability to optimize spatial efficiency while maintaining high energy production. The novelty of this work lies in its tailored simulation approach, addressing the unique geometry and operational dynamics of the V-shaped configuration, and its potential adaptability to diverse agrivoltaics scenarios. Unlike existing tools and methodologies in the literature, this work introduces a customized Python-based model specifically designed to analyse the performance of this innovative structure, which is of recent conception and lacks precedent in both academic studies and commercial software solutions. By advancing the methodological framework for integrating renewable energy with agriculture, this study contribute to the broader goals of sustainable development and climate resilience.

1. Introduction

The transition from fossil fuels to renewable energy is driven by the need to reduce greenhouse gas emissions, combat climate change, and enhance energy security. The Conference of the Parties (COP) annually reviews climate initiatives and sets new goals aligned with the Paris Agreement, which aims to limit global warming to 1.5 °C above pre-industrial levels [1].

At COP28, the urgency for climate neutrality was highlighted, with calls to phase out fossil fuels, triple renewable energy capacity to over 11

* Corresponding author.
E-mail addresses: stefania.guarino@unipa.it (S. Guarino), alessandro.buscemi@unipa.it (A. Buscemi), c.chiaruzzi@horizonfirm.com (C. Chiaruzzi), valerio.lobrano@unipa.it (V. Lo Brano).

https://doi.org/10.1016/j.apenergy.2025.125785
Received 10 December 2024; Received in revised form 23 January 2025; Accepted 19 March 2025
0306-2619/© 2025 The Authors. Published by Elsevier Ltd. This is an open access article under the CC BY license (http://creativecommons.org/licenses/by/4.0/).

TW, and double energy efficiency improvements by 2030 [2]. COP29 in Baku reaffirmed these goals, advancing carbon markets under Article 6 of the Paris Agreement, increasing climate finance for developing nations, and strengthening adaptation and resilience strategies. Enhanced climate reporting through the Transparency Framework also set the stage for more robust global policies [3].

Despite the measures implemented to support the energy transition, fossil fuels still dominate global electricity production. In 2023, approximately 60.6 % of global electricity was generated using fossil fuels, 30.2 % came from renewable energy sources, and the remaining 9.1 % came from nuclear power [4,5]. In the same year, renewable energy accounted for 43 % of the global power capacity, driven by an impressive annual growth of 473.4 GW. Of this, solar photovoltaic (PV) systems alone contributed 345.5 GW, highlighting their pivotal role in the expansion of renewables worldwide [6]. Reflecting this growth, the global weighted average Levelized Cost of Electricity (LCOE) for utility-scale solar PV plants decreased significantly by 90 % between 2010 and 2023, dropping from USD 0.460 to USD 0.044 per kWh. In 2023 alone, a further year-on-year reduction of 12 % was observed, highlighting continuous advancements in solar PV cost efficiency [7].

According to data published in a report by the International Renewable Energy Agency (IRENA), solar photovoltaic, hydropower, and wind energy are currently the leading renewable technologies, with their installed capacities globally distributed almost equally. Moreover, projections under the 1.5 °C Scenario anticipate significant growth for solar PV. By 2030, its installed capacity is expected to increase from 1411 GW in 2023 to 5457 GW, accounting for 48.8 % of the total renewable capacity, which is projected to reach 11,174 GW globally [8].

Meeting these ambitious targets and supporting the energy transition requires large-scale deployment of solar PV systems. This calls for accelerated investments, supportive policies, and optimized land and resource use to ensure sustainable and efficient installation. While utility-scale energy PV systems stand out for their environmental advantages, in particular low-carbon electricity production, they also introduce complex challenges that need careful consideration [9]. One significant issue is the potential reallocation of land, which could divert areas from agricultural use or alter natural habitats. The installation of utility-scale PV plants has the potential to disturb local and regional biodiversity through habitat disruption and landscape fragmentation [10,11]. Regarding water usage, photovoltaic systems generally require minimal amounts for maintenance such as panel washing and dust control [12]. However, even this limited use can significantly affect the hydrology of arid regions already experiencing high levels of water stress. In addition, the construction and maintenance of solar farms may lead to soil compaction, erosion, and depletion of organic carbon stocks in the soil, especially when vegetation is cleared to accommodate solar installations [10,11].

Utility-scale PV system installations modify surface albedo and, consequently, the amount of sunlight reflected by the Earth's surface [13,14]. Ice caps, being high-albedo surfaces, reflect most of the sunlight, whereas lower-albedo surfaces, like forests or open fields, absorb more [15]. PV panels, designed to directly convert solar energy into electricity, feature high absorption coefficients [16], resulting in lower albedo compared to the natural or uncultivated land they replace. The alteration in albedo caused by PV systems can influence local and regional climates by changing the amount of solar energy reflected into the atmosphere, potentially increasing local temperatures [17]. This effect, known as the photovoltaic heat island effect, has the potential to significantly affect both local ecosystems and climatic patterns [18]. It is crucial to highlight that while solar energy exhibits resilience against climate change [19], expected temperature rises might reduce its efficiency, with projections indicating a drop of up to 12 % by 2050 [20].

Agrivoltaic systems (APV), which combine the co-location of agriculture and solar PV panels, present a promising solution to alleviate some of the challenges associated with traditional utility-scale solar farms [21]. These systems can enhance land profitability while shielding crops from excessive heat and moderating soil temperatures. Additionally, the shade under the solar panels reduces evaporation from the soil and plant leaves, allowing for more conservative water use [22]. Factors affecting crop production in APV systems include air temperature, humidity, wind speed, soil moisture, and crop temperature. Together with the shading from solar panels, these elements help optimize crop growth, enhance water use efficiency, and reduce environmental stress [23]. Recent advancements in photovoltaic modelling have also contributed to optimizing performance under diverse conditions. Yadav et al. analysed single- and multi-diode models, evaluating factors such as irradiation, temperature, and shading effects, and provided insights into improving PV module performance [24]. Similarly, advanced optimization algorithms, like those presented by Abdullah et al., have enhanced maximum power point tracking (MPPT) techniques for grid-connected systems, improving operational efficiency under variable environmental conditions [25]. While these methods offer significant contributions to photovoltaic performance optimization, they are not tailored to the unique challenges posed by agrivoltaic configurations, particularly systems integrating bifacial modules in innovative geometries.

A key factor in APV systems is selecting crops that can tolerate shaded conditions created by solar panels. Shade tolerance is assessed through photosynthesis-light response curves, which show how a plant's photosynthesis rate responds to varying light levels. From these curves, the light saturation point is identified, representing the maximum light intensity the plant can efficiently use for photosynthesis [26]. Exceeding this threshold can lead to photoinhibition, where the plant limits light absorption to prevent damage [27]. This challenge is particularly pronounced in regions like the Mediterranean, where high summer irradiance and temperatures can negatively impact crops such as olive trees [28]. Combining the optimal spatial configuration of agrivoltaic systems with the specific crops they integrate [29,30], while balancing crop growth requirements and energy production, is essential to maximize land-use efficiency and support sustainable agriculture [31,32]. A recent study on agrivoltaic systems for pear orchards in Belgium demonstrated the potential of integrating PV modules with existing agricultural layouts to balance energy production and crop protection. The study addressed challenges such as shading impacts, cost-effectiveness, and system design optimization under fixed geometrical constraints. It reported a specific energy yield of 950 kWh/kWp (570 MWh/ha) and a favourable microclimatic effect, such as frost protection, though it resulted in a slight 16 % reduction in pear yield due to fewer and smaller fruits [33].

APV systems can be classified based on several factors, such as the system type, structure, module tilt, and application. They can either be open or closed systems, with open systems typically used in open-field farms, and closed systems applied in protected environments like greenhouses. The structure can include interspace PV, where panels are installed between crops (suitable for grassland and arable farming), or overhead PV, placed above crops (ideal for horticulture). Further classification is based on the tilt of modules, which may be fixed or adjustable, using one-axis or two-axis tracking systems. The application also varies across different farming types, including grassland farming, arable farming, horticulture, and aquaculture. While some agrivoltaic systems, such as those used in animal husbandry under closed opaque buildings, are not typically classified as agrivoltaics, they represent an interesting variant in the broader landscape [34]. Despite their promise, agrivoltaic systems are still evolving, with significant room for technical advancements and adaptation across various agricultural sectors. However, challenges such as long-term land productivity, market potential, and system flexibility remain barriers to widespread adoption, though these can be mitigated through strategic planning and cooperation between the solar and agricultural sectors.

In recent studies, the integration of photovoltaic systems into vineyards is emerging as a promising solution to simultaneously support agricultural production and renewable energy generation. Vertical PV

installations on grape trellises minimize land use, reduce visual impact, and maintain crop productivity, achieving energy efficiency comparable to ground-mounted systems while providing minimal shading [35]. A techno-economic analysis in India demonstrated that such systems could increase farm revenue by up to 15 times without compromising grape yields [36], illustrating their potential to resolve land-use conflicts through dual land utilization. In vineyard applications, APV systems alter the microclimate, reducing air and soil temperatures by 1–2 °C, which enhances soil moisture retention and mitigates water stress. A three-year study in Northern Italy with *Vitis vinifera* L. cv. Corvina found that APV systems improved vine resilience during the midday heat, with higher transpiration and photosynthesis rates compared to full-sun vines. While yield reductions were minor, grape quality parameters such as anthocyanins and polyphenols slightly decreased. These results underscore the potential of APV systems to enhance land productivity in arid and hot climates under changing climate conditions. Moreover, an innovative platform was developed to optimize agrivoltaic systems, combining electricity generation with crop production. Long-term simulations showed that these systems can support higher agricultural productivity, particularly under drought stress conditions, while also contributing to water conservation and clean energy production [37,38].

Sun tracking systems, particularly when combined with bifacial PV technology, are essential in agrivoltaics for optimizing solar energy production while balancing light conditions for crop growth, thereby improving both energy yield and agricultural productivity. Hussain and Ghosh emphasize that geographical location and PV configuration significantly influence agrivoltaic system performance, with bifacial tracking systems generating higher energy output but potentially reducing crop yields, making the selection of an appropriate location crucial for optimizing system performance [39]. Additionally, Willockx et al. note that single-axis tracking systems in interspersed agrivoltaic setups offer higher energy production and lower levelized cost of energy compared to vertical configurations, though challenges such as land loss and crop yield reductions must be addressed for successful integration with agriculture [40]. Furthermore, Patel et al. demonstrate that East/West single-axis tracking bifacial PV farms can yield up to 45 % more energy annually than North/South fixed-tilt bifacial farms in regions within 30 degrees of the equator, optimizing land use and light capture efficiency. Their findings suggest that bifacial tracking systems, which adjust dynamically to solar paths, significantly enhance solar energy production, making them the preferable choice for maximizing PV energy output across various geographic settings [19].

This study aims to estimate the energy production of an innovative photovoltaic system configuration, which integrates bifacial photovoltaic modules and is specifically designed for agrivoltaic applications. While various methods for simulating photovoltaic system performance exist in the literature, these approaches lack the flexibility to address the unique geometric and operational features of the patented V-shaped bifacial photovoltaic configuration. This new system, developed and patented by the Horizonfirm S.r.l. Italian company, is characterized by bifacial modules arranged in a V-shape with a tracking system. The energy production of this new configuration has been evaluated through the implementation of a newly developed solar tracking algorithm. In fact, no algorithms or tools are currently available in the literature that can directly simulate the performance of this unique panel V-shaped configuration. The newly developed model considers mutual shading effects between the two modules forming the V-shaped configuration. It also accounts for the fraction of solar radiation that reflects multiple times within the cone structure created by the panels. Additionally, it estimates the solar radiation reflected from the underlying surface that irradiates the back of the panels, taking full advantage of the bifacial module design. The system under study also features a single-axis solar tracking mechanism that allows the slope of the modules to be modified equally and according to the solar elevation, with a lower limit of 50°. These features required a model that dynamically evaluates solar radiation as input to the PV system. The model also considers variations in the cone's aperture based on the solar position. To this end, a custom algorithm was developed in Python, harnessing the advanced functionalities of the *PVlib* library [41–43]. Specifically tailored to simulate the operational dynamics of the V-shaped bifacial photovoltaic configuration, the algorithm enables precise modelling of key parameters such as solar position, plane-of-array (POA) irradiance, mutual shading effects, and multiple radiation reflections within the system. By integrating Python and *PVlib,* the model gains flexibility, scalability, and adaptability. This makes it suitable for various system configurations and geographic locations. This innovative approach led to the development of an open, generalizable, and reliable tool for accurately estimating the energy production of bifacial photovoltaic panels in this novel arrangement. Furthermore, it facilitates comprehensive assessments of the economic feasibility of the proposed setup compared to conventional configurations currently available on the market.

The paper is structured as follows: Section 2 presents the materials and methods implemented to conduct the study, including the definition of the newly proposed bifacial configuration with a solar tracking system, a description of the model developed to simulate the operation of the solar tracking system, and the estimation of the solar radiation captured by the examined system. This section also defines the case study, and the comparative analysis carried out. Section 3 presents and discusses the results obtained in terms of energy producibility for the various analysed scenarios. Finally, Section 4 presents the conclusions of the study.

1.1. Objectives of the study and motivation

The primary objective of this manuscript is to evaluate the energy performance and land use efficiency of an innovative agrivoltaic system that integrates bifacial photovoltaic modules arranged in a patented V-shaped configuration. Specifically, the study aims to:

- Develop a custom Python-based simulation model tailored to the unique geometry and operational dynamics of the V-shaped system, addressing limitations in existing tools.
- Quantify the energy production and land-use optimization achieved by this configuration under real-world climatic conditions, using Palermo, Italy, as a case study.
- Assess the adaptability of the proposed model to various agrivoltaic designs and geographic locations, highlighting its potential as a generalizable and scalable tool for sustainable energy applications.
- Demonstrate the practical benefits of this novel system in balancing renewable energy generation with agricultural productivity, while adhering to regulatory standards.

By addressing these objectives, the manuscript contributes to advancing the state-of-the-art in agrivoltaic system design and analysis, offering insights for future research and real-world implementations.

1.2. Novelties and contributions of the work

This study presents a novel approach to agrivoltaic systems, combining innovative design and advanced modelling techniques to address key challenges in integrating renewable energy with agriculture. The research focuses on a patented V-shaped configuration of bifacial photovoltaic modules, equipped with a single-axis solar tracking mechanism [44]. This unique design dynamically adjusts the panel tilt to optimize energy capture by reducing shading effects and enhancing the contribution of both direct and reflected solar radiation. This approach not only improves energy yield but also supports agricultural activities by preserving land availability and reducing environmental impacts.

A major contribution of this work is the development of a custom Python-based simulation model, utilizing the PVlib library. Unlike

existing tools, this model is specifically tailored to the V-shaped configuration. It incorporates detailed calculations of mutual shading, multiple reflections within the cone structure, and ground albedo effects. By dynamically adjusting panel slopes based on solar elevation, the model provides accurate and realistic assessments of system performance under various climatic and operational conditions. This tool represents a significant advancement in the modelling of complex PV systems, offering a framework adaptable to different configurations.

The study also contributes to the practical implementation of agrivoltaic systems, by aligning the design with the Italian regulations that emphasize the dual objectives: renewable energy production and agricultural preservation. By maintaining low ground coverage ratios and ensuring compatibility with vineyard cultivation, the proposed system demonstrates its feasibility and adaptability for real-world applications. Furthermore, the results highlight the potential of the V-shaped configuration to outperform traditional fixed-tilt bifacial systems, particularly in regions with high solar irradiance. This improvement in energy efficiency, combined with minimal impact on agricultural productivity, underscores the system's value as a sustainable solution for integrated energy and agricultural production.

By addressing both the technical and practical aspects of agrivoltaic systems, this work advances the state of the art, paving the way for further innovations and contributing to the broader transition toward sustainable energy and land-use practices.

1.3. Italian regulatory framework for agrivoltaics

The Italian regulatory framework for agrivoltaics, established by the Ministry of Ecological Transition, defines a comprehensive set of criteria to promote the integration of agricultural activities with renewable energy production. To qualify as agrivoltaic, systems must meet specific requirements, including the simultaneous execution of agricultural and photovoltaic activities (Requisite A) and the maintenance of both agricultural and energy production throughout the system's lifecycle (Requisite B). Advanced agrivoltaic systems are further required to adopt innovative technical solutions, such as elevated panels that minimize land-use conflicts and optimize agricultural operations (Requisite C). Additionally, monitoring tools must assess impacts on crop yields, water use efficiency, and agricultural productivity (Requisite D), along with systems to evaluate changes in soil fertility and microclimatic conditions (Requisite E) [45].

The framework also establishes quantitative thresholds, such as maintaining at least 80 % of agricultural productivity and limiting photovoltaic coverage to a maximum of 40 % of the total agricultural area. For perennial crops like vines, agrivoltaic installations can serve as a climate adaptation strategy, mitigating heat stress and reducing water evaporation. Furthermore, the system power density, typically measured in kW per hectare, must ensure a balance between energy generation and agricultural preservation. This study investigates how innovative photovoltaic configurations, including bifacial V-shaped systems, can address these challenges while adhering to Italian regulatory standards [45].

2. Material and methods

This section details the components, configuration, and methodology employed to assess the energy performance of the V-shaped configuration in the examined agrivoltaic system. The study integrates an innovative structural arrangement of bifacial photovoltaic modules with a newly developed solar tracking algorithm. Key aspects, including system setup, modelling parameters, and simulation techniques, are thoroughly outlined to ensure reproducibility and provide insights into the specific operating conditions of the system.

2.1. System configuration and bifacial module specifications

This study evaluates the energy production of the V-shaped PV system, a recent innovation patented and designed by Horizonfirm S.r.l [44]. This state-of-the-art system employs bifacial modules in a novel configuration, distinguishing it from conventional designs. As illustrated in Fig. 1, the system features two identical bifacial photovoltaic modules arranged in a sub-vertical V-shape, facing each other. The module slopes can dynamically adjust from a minimum of 50° to a maximum of 90°, depending on solar elevation. In this setup, the apex line of the V-shaped cone is positioned 3 m above the ground, with one module, for instance, oriented eastward (azimuth = 90° - Panel 1) and the other westward (azimuth = 270° - Panel 2). This arrangement enables the panels to capture sunlight at different times of the day, effectively distributing solar exposure between morning and evening hours. The azimuth angle of each panel is a fixed operational parameter that can be chosen appropriately, as this configuration does not include an azimuthal tracker.

2.2. Single-axis solar tracking and radiation modelling

The analysed bifacial PV system comprises two bifacial modules with a fixed azimuthal orientation, mounted on a single-axis solar tracking system. This system automatically adjusts the panels' tilt in response to changes in solar elevation, thereby optimizing the absorption of solar irradiation. As no existing tools or commercial software can dynamically simulate this specific configuration, a custom Python algorithm was developed to meet this need. The choice of a Python-based approach was motivated by its flexibility and ability to accommodate the unique geometric and operational features of the V-shaped bifacial configuration. Leveraging libraries such as numpy, pandas, and PVlib [46], the algorithm enables simulations based on weather data for the selected location, as well as the geometric and technical specifications of the panels. Specifically, it calculates the solar position, and the Plane-of-Array (POA) irradiance [47] on the cone surfaces, while accounting for mutual shading between the panels, multiple radiation reflections within the cone, and the system production, including the effects of module temperature.

To implement this model, three Python scripts were developed: a *Functions Module*, an *Irradiance Calculation* script, and an *Optimal Orientation Calculation* script. Each script performs a specific role in structuring and executing the simulation:

1. *Functions Module*: This module acts as a core library, hosting the primary procedures and functions required for irradiance calculations, mutual shading assessment, and accounting for multiple reflections between the panels. By standardizing and centralizing these recurring operations, this module ensures consistency and provides accessible functionalities for the other scripts.
2. *Irradiance Calculation* script: This script utilizes the functions from the support module to simulate irradiance on the system, dynamically adjusting the panel tilts based on solar elevation. Both panels uniformly modify their tilt according to changes in solar position, following the operational principles of the novel bifacial photovoltaic system configuration under analysis. By leveraging clear-sky data or TMY data, the script estimates the POA irradiance with and without shading, including the effects of mutual shading and multiple reflections within the cone. It also computes module temperature and power output using the Faiman model [48], considering bifaciality and temperature coefficients. Ultimately, providing an estimate of annual energy production.
3. *Optimal Orientation Calculation* script: This script determines the optimal cone orientation by iterating over different azimuth angles to maximize total irradiance captured by the system and thereby enhancing energy production.

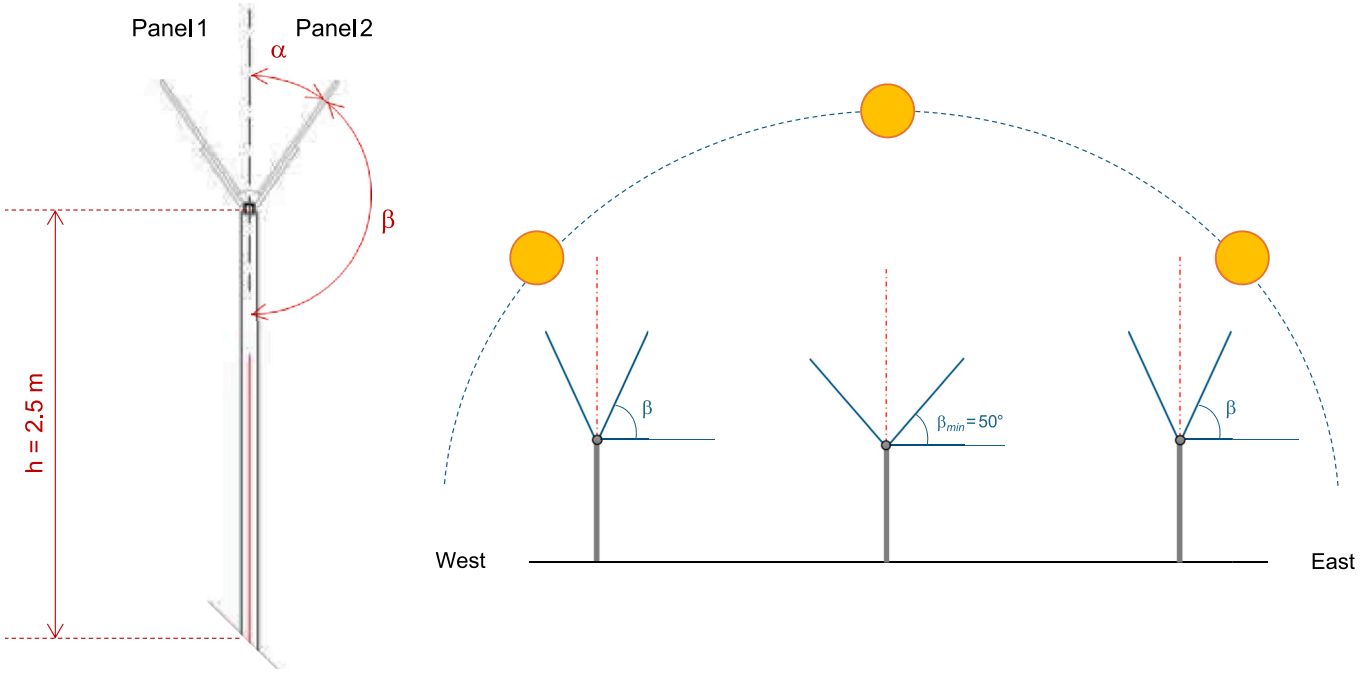

Fig. 1. Schematic representation of the examined PV system configuration: two bifacial photovoltaic modules arranged in a V-shape, equipped with a single-axis tracking mechanism.

Together, these scripts enable a comprehensive simulation of irradiance and power generation, particularly suited for analysing bifacial PV configurations in agrivoltaic systems.

The algorithm's core lies in the calculation of POA irradiance, which accounts for mutual shading and multiple reflections within the cone structure, including up to the fourth reflection, to accurately evaluate contributions to useful irradiance. Below is a breakdown of how mutual shading and reflections are incorporated into the POA irradiance calculations:

a. Mutual shading between modules

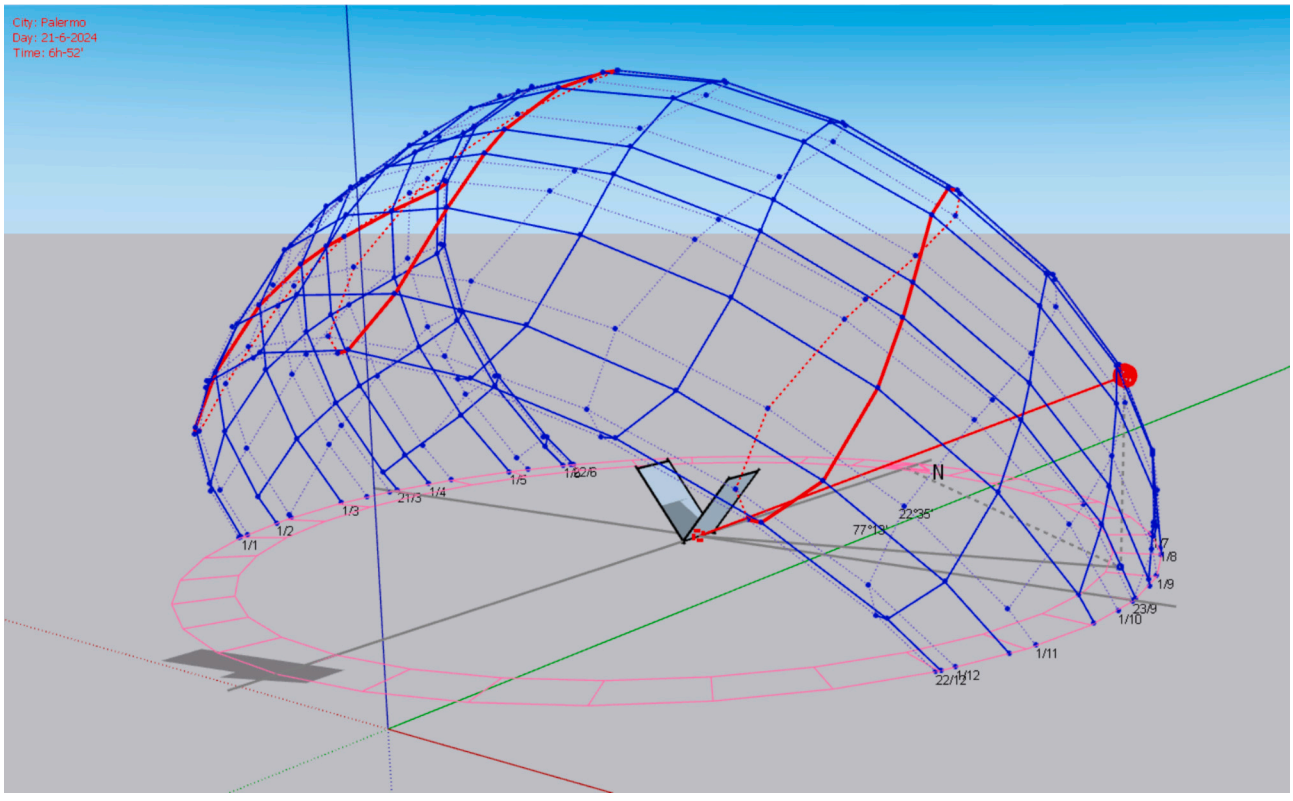

Fig. 2. Mutual shading between bifacial modules in the V-shaped configuration.

The modules, arranged in a V-shaped configuration, exhibit mutual shading, which is addressed as follows:

- *Dynamic tilt adjustment*: In the *Irradiance Calculation* script, the tilt angle of each module is dynamically adjusted based on the solar position to maximize sunlight capture. This adjustment allows the modules to open or close relative to each other while maintaining a fixed bisector perpendicular to the ground. This consistent alignment ensures efficient energy collection throughout the day by optimizing the system's orientation to the sun.
- *Shading calculation:* At specific times of the day, one module partially shades the opposite module, as illustrated by the shading pattern visible on the module surface in Fig. 2. The shading effects between the two modules are calculated using the Shadow function from the *Functions Module* script. This function computes shading fractions of each module by evaluating parameters such as the tilt angle, height, width, azimuth of the panels, and solar position. These shading fractions are then applied to adjust the global solar irradiance values through the pvlib.irradiance.get_total_irradiance calls [49], effectively integrating the impact of mutual shading into the irradiance received by each module.

b. POA irradiance calculation with shading and reflections

To accurately calculate the irradiance on the Plane of Array (POA), the code follows these steps:

- *Initial POA calculation with shading:* For each panel, the initial POA irradiance is calculated using pvlib.irradiance.get_total_irradiance [49]. This function considers key factors such as the panel's tilt, azimuth, direct normal irradiance (DNI), global horizontal irradiance (GHI), diffuse horizontal irradiance (DHI), and solar position. These calculations are performed for both shaded and unshaded conditions to evaluate the impact of mutual shading on direct irradiance. The direct POA components (POAS for Panel 1 and POAN for Panel 2) are extracted and used as the basis for subsequent reflection calculations.
- *Shading impact assessment:* Ratios of shaded to unshaded direct irradiance are computed to quantify the shading effect on the irradiance received by each panel. This step ensures that the reduction in direct solar radiation due to shading is accurately accounted for in the model.
- *Angle of incidence (AOI) determination and IAM calculation:* The angle of incidence for each panel – aoiS for Panel 1 and aoiN for Panel 2 – is determined based on the panel's tilt, azimuth, and the solar position. Using the physical Incidence Angle Modifier (IAM) model (pvlib.iam.physical [50]), an IAM factor is calculated for each AOI. This calculation incorporates the panel refractive index, extinction coefficient, and glazing thickness, representing the loss of irradiance due to reflection. By including both shading effects and angular losses, the calculation achieves a high degree of accuracy in estimating the irradiance on the panels.
- *Reflections inside the cone*: Reflections within the cone structure are simulated up to the fourth reflection to accurately model their cumulative effect on the POA irradiance. The calculation is performed iteratively with the POA for each subsequent reflection being determined based on the preceding reflection. For each reflection, the AOI of the reflected ray on the opposite panel is calculated. For instance, the AOI for the first reflection on Panel 2 is derived from the angle of incidence of the reflected ray originating from Panel 1. This step ensures that the geometric relationship between the panels is accurately captured for each successive reflection. Based on the AOI of each reflection, an IAM is computed. This factor accounts for the reduction in irradiance due to reflection losses, incorporating the optical properties of the panel. These calculations are iteratively applied for each subsequent reflection to assess the cumulative impact on the total POA irradiance: The initial reflected irradiance from each panel is calculated using the direct irradiance received on the panel and the reflection losses determined through the IAM factor:

$$POA1_0 = POAS \cdot (1 - IAM1) \tag{1}$$

$$POA2_0 = POAN \cdot (1 - IAM2) \tag{2}$$

where:

- $POA1_0$ and $POA2_0$ indicate the initial reflected irradiance originating from Panel 1 and Panel 2, respectively, representing the portion of solar radiation reflected by each panel's surface.
- POAS and POAN represent the initial direct POA irradiance values incident on Panel 1 and Panel 2, respectively, accounting for the direct solar radiation received by each panel.
- IAM1 and IAM2 represent the incidence angle modifiers for the initial reflections on Panel 1 and Panel 2, respectively, quantifying the reduction in reflected irradiance due to the angular dependence of the panels' optical properties.

For each subsequent reflection ($n \geq 1$), the POA irradiance contribution from each reflection is then calculated iteratively. This is achieved by multiplying the POA from the previous reflection ($n-1$), by the IAM factors corresponding to the current and previous reflections, simulating the cumulative energy reduction resulting from repeated bounces. The general formulas for the POA contribution at each reflection level are:

$$POA1_n = POA2_{n-1} \cdot (1 - IAM2_{n-1}) \cdot (1 - IAM1_n) \tag{3}$$

$$POA2_n = POA1_{n-1} \cdot (1 - IAM1_{n-1}) \cdot (1 - IAM2_n) \tag{4}$$

In these equations:

- $IAM1_n$ and $IAM2_n$ represent the incidence angle modifiers for the n-th reflection on Panel 1 and Panel 2, respectively.

For each panel, the contributions of successive reflections are systematically calculated and stored. This ensures that all reflected components, up to the fourth reflection, are included in the total POA irradiance. This iterative approach captures the intricate dynamics of light reflection within the V-shaped structure, providing a detailed simulation of the system's optical behavior.

- *Total POA calculation*: The total direct POA irradiance for each panel ($POA_{total,1}$ and $POA_{total,2}$) is computed by summing the direct POA irradiance with the contributions from all subsequence reflections. For Panel 1, the total POA is expressed as:

$$POA_{total,1} = POAS + POA_{1S} + POA_{2S} + POA_{3S} + POA_{4S} \tag{5}$$

Similarly for Panel 2:

$$POA_{total,2} = POAN + POA_{1N} + POA_{2N} + POA_{3N} + POA_{4N} \tag{6}$$

In these equations:

- POAS and POAN represent the initial direct POA irradiance on Panel 1 and Panel 2, respectively.
- POA_{1S}, POA_{2S}, POA_{3S}, and POA_{4S} are the contributions from the first, second, third, and fourth reflections on Panel 1, respectively.
- POA_{1N}, POA_{2N}, POA_{3N}, and POA_{4N} are the contributions from the first, second, third, and fourth reflections on Panel 2, respectively.

Each term accounts for the direct POA irradiance and the incremental contributions from successive reflections, capturing the cumulative effect of light interactions within the V-shaped structure. This

approach ensures a comprehensive evaluation of the total energy incident on the panels.

c. Final absorbed POA and temperature adjustments

- *Absorbed irradiance with multiple reflections:* The absorbed irradiance is calculated as the sum of all contributions from direct irradiance and successive reflections. This aggregate value serves as the basis for further calculations, including the assessment of temperature effects on the modules through pvlib.temperature.faiman function [51]. This model estimates the temperature of the module as a function of total incident irradiance, ambient dry-bulb temperature, wind speed, and heat loss factors, including thermal resistance and convective cooling parameters [48]. By integrating the Faiman model with the irradiance data, the algorithm accurately reflects the interplay between irradiance levels and module operating temperatures, capturing the thermal behavior of the system under varying environmental conditions.

This modelling approach ensures a realistic simulation of irradiance effects by integrating mutual shading and multiple reflections specific to the cone configuration. These factors are meticulously incorporated into the irradiance calculation for each module, enabling precise estimation of energy production. It is important to note that the calculation of the module's energy production does not account for the electrical connections between individual cells. Instead, the POA irradiance is proportionally adjusted based on the percentage of the shaded surface area.

To enhance clarity regarding the methodology and code structure, a block diagram is provided in Fig. 3. This diagram illustrates the sequential steps and interactions within the developed scripts for simulating irradiance and power output in a bifacial PV system with a single-axis tracking mechanism. Each block in the diagram represents a critical element of the simulation process, including:

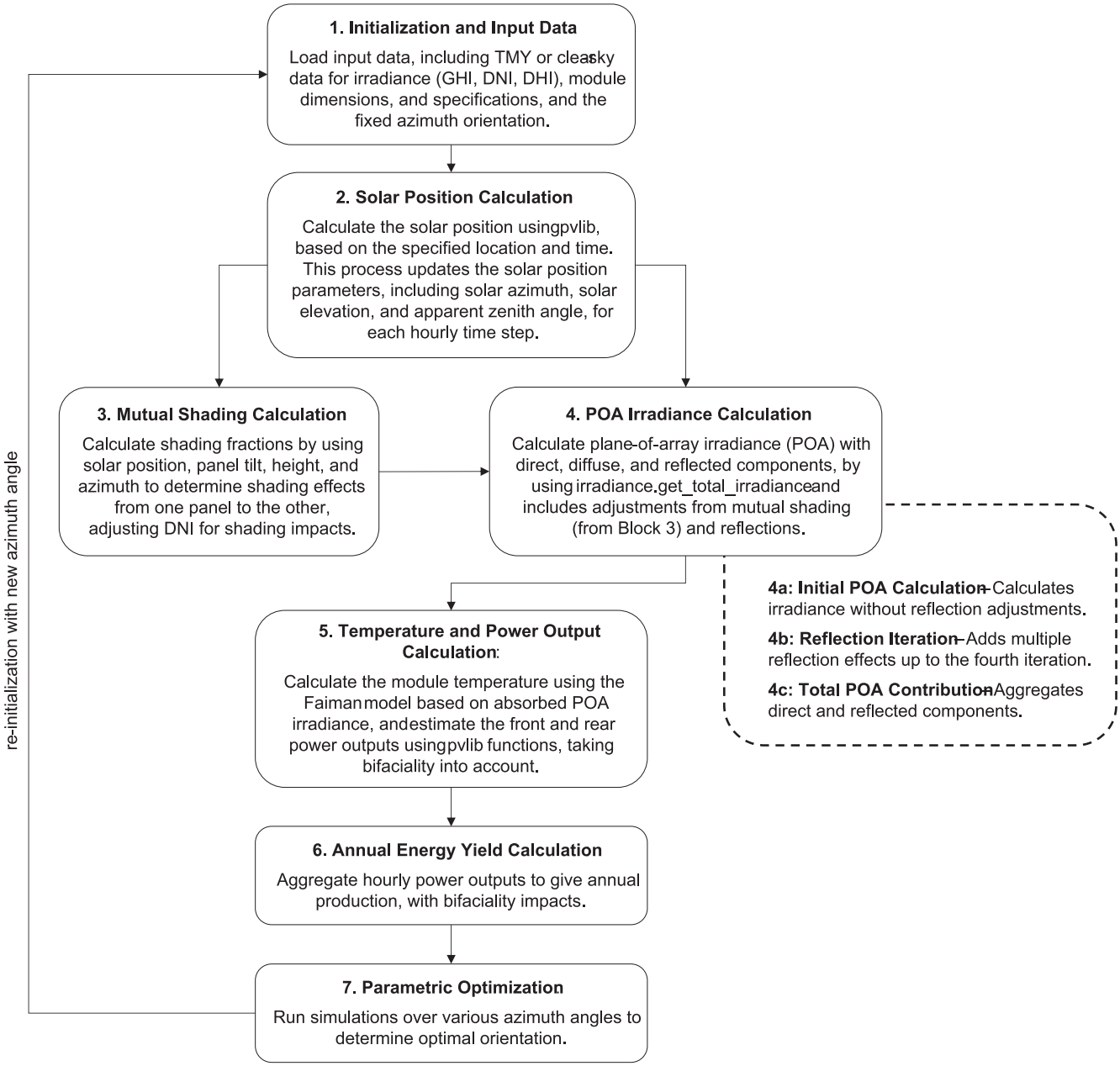

Fig. 3. Block diagram outlining the methodology for calculating irradiance and power in a bifacial PV system.

- initial setup and solar position calculation;
- shading analysis to assess mutual shading effects;
- computation of irradiance, incorporating both direct and reflected components;
- parametric optimization of azimuth angles to maximize energy yield.

This visualization underscores the integration of shading and multiple reflection effects, highlighting their significance for accurately modelling bifacial PV systems in an agrivoltaic context.

2.3. Details of the case study configuration and comparative analysis

For the V-shaped configuration agrivoltaic system, the TrinaSolar Vertex bifacial dual glass monocrystalline PV module (model: TSM-DEG21C.20) was selected. This module delivers a peak power output of 665 W and features dimensions of 2384 mm in length, 1303 mm in width, and 33 mm in thickness [52]. By leveraging high-density interconnect technology, the modules achieve an efficiency of up to 21.4 %. They are characterized by a lower temperature coefficient of −0.34 % and an optimal operating temperature range. Additionally, under optimal albedo conditions, the bifacial design allows for up to 25 % additional power from the backside. The technical specifications for this module are detailed in Table 1 [52].

For this study, the installation site is located in Palermo, Italy (latitude: 38.1°, longitude: 13.38°), a southern city with a distinctive Mediterranean climate. Data from the Typical Meteorological Year (TMY), generated by Meteonorm for Palermo, highlights seasonal trends in both global horizontal irradiance (GHI) and dry-bulb air temperature. The GHI follows a pronounced seasonal pattern with peak monthly cumulative values during the summer months, particularly in June and July, driven by longer daylight hours and stronger solar radiation. In contrast, during the winter months, like December and January, GHI values drop significantly. This variation reflects the Mediterranean climate, where abundant summer sunlight contrasts with the reduced solar availability in winter, yielding an annual solar irradiation value of 1629.9 kWh/m^2 (see Table 2). Temperature trends also align with these seasonal variations. July and August record the highest average temperatures ranging from 28 to 30 °C, while December and January feature milder conditions, with averages around 13–15 °C and less variability between daily minimum and maximum temperatures. As summarised in Fig. 4, the mean annual GHI is 186 W/m^2 with a peak of 1132 W/m^2, while mean air temperatures reach 20.1 °C, peaking at 38.4 °C. These statistics provide a comprehensive understanding of the solar resource and temperature distribution, confirming Palermo's suitability for solar energy applications.

The data reported in Table 2 suggest that Palermo's climate offers highly favourable conditions for solar energy generation, particularly during the summer months when solar irradiance peaks, enhancing the efficiency of solar installations. The V-shaped configuration system, with its dual-sided bifacial design, is particularly well-suited to this climate. Its ability to capture both reflected and diffuse light ensures optimized energy production, even during periods of low solar elevation. This setup is designed to maximize energy capture in the morning and evening hours, adapting effectively to the daily and seasonal variations in the solar path characteristic of this location. Moreover, the study hypothesises that the V-shaped photovoltaic technology can be successfully integrated into the agrivoltaic sector, particularly with crops like vines, which are widely cultivated in Sicily.

To evaluate the impact of the V-shaped configuration on land-use efficiency, the system was compared with an alternative configuration using the same bifacial PV modules arranged conventionally. As illustrated in Fig. 5, the conventional configuration positions the modules with optimal azimuth and tilt angles for the selected location (β_2 and β_3 equal to latitude). Modules in the conventional setup could be placed either side by side (see Fig. 5.b) or in a row-to-row configuration where one module is positioned behind the other (see Fig. 5.c). These scenarios were analysed to highlight differences in the land area required for installation, providing insights into the comparative efficiency of the proposed V-shaped configuration system.

For each scenario, the Ground Coverage Ratio (GCR) was calculated to evaluate and compare land-use efficiency. This metric incorporates key parameters such as the dimensions of the PV panels - length (L) and width (W) – along with their tilt angle (β_i) and the spacing between them (d). The GCR is commonly defined as the ratio of the total length of the PV array (L') and the minimum distance between successive rows (R),

Table 1
Technical specifications of the bifacial dual glass monocrystalline PV modules used in the V-shaped configuration (model: TSM-DEG21C.20) [52].

Specification	Value
Electrical data (STC)	
Peak Power Watts - P_{max}	665 W_p
Power Tolerance - P_{max}	0 ∼ +5 %
Maximum Power Voltage - V_{MPP}	38.3 V
Maximum Power Current - I_{MPP}	17.39 A
Open Circuit Voltage - V_{OC}	46.1 V
Short Circuit Current - I_{SC}	18.5 A
Module Efficiency	21.4 %
Electrical data (NOCT)	
Maximum Power Voltage - V_{MPP}	35.6 V
Maximum Power Current - I_{MPP}	14.16 A
Open Circuit Voltage - V_{OC}	43.4 V
Short Circuit Current - I_{SC}	14.91 A
Mechanical data	
Solar cells type	Monocrystalline
Number of cells	132 cells
Module dimensions	2384 × 1303 × 33 mm
Weight	38.3 kg
Front glass	High transmission, AR Coated Heat Strengthened Glass
Encapsulant material	POE/EVA
Back glass	2.0 mm - Heat Strengthened Glass (White Grid Glass)
Frame	33 mm - Anodized Aluminium Alloy
Optical properties of the glass	
Refractive index	1.3
Extinction coefficient	4 m^{-1}
Glazing thickness	2.0 mm
Temperature ratings	
NOCT (Nominal Operating Cell Temperature)	43 °C (±2)
Temperature Coefficient of P_{MAX}	−0.34 %/°C
Temperature Coefficient of V_{OC}	−0.25 %/°C
Temperature Coefficient of I_{SC}	0.04 %/°C

Table 2
Monthly average, maximum and cumulative values of GHI.

Month	$GHI_{average}$	GHI_{max}	Monthly cumulative GHI
	[W/m^2]	[W/m^2]	[kWh/m^2]
January	79.9	53	59.4
February	114.9	655	77.2
March	172.0	819	128.0
April	226.0	924	162.7
May	276.8	1027	205.9
June	293.0	1012	211.0
July	296.9	1132	220.9
August	264.9	935	197.1
September	197.8	882	142.4
October	143.9	809	107.1
November	90.9	594	65.5
December	70.9	497	52.7
Annual			**1629.9**

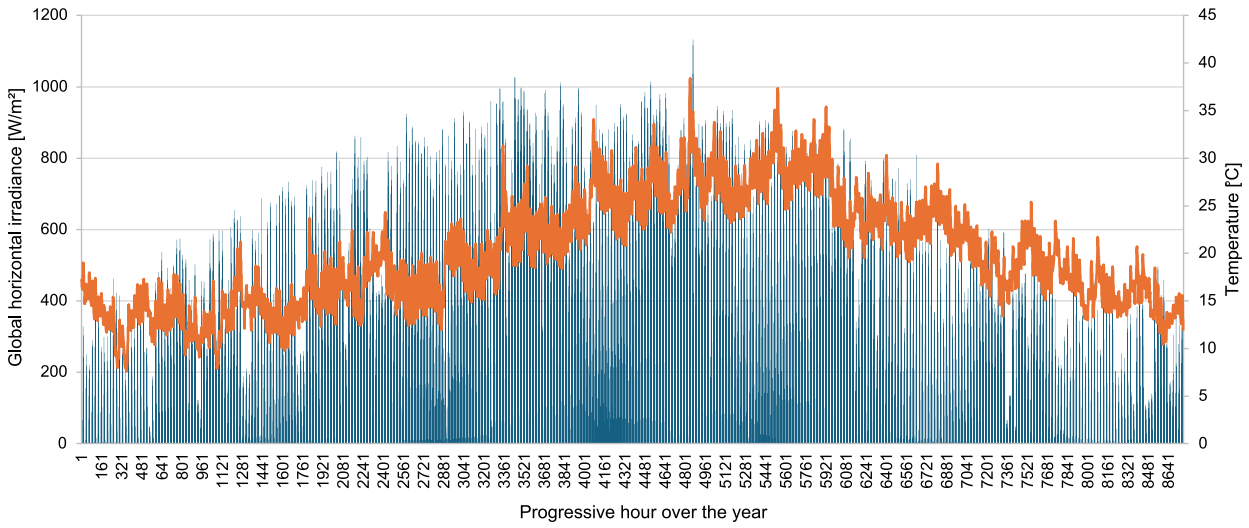

Variable	Count	Mean	Standard deviation	Min	25th Percentile	Median	75th Percentile	Max
GHI	8760	186.06	266.02	0	0	3	331	1132
T_{air}	8760	20.09	5.81	7.6	15.2	19.5	24.5	38.4

Fig. 4. Hourly data of global horizontal irradiance and dry-bulb air temperature over the year (data from TMY).

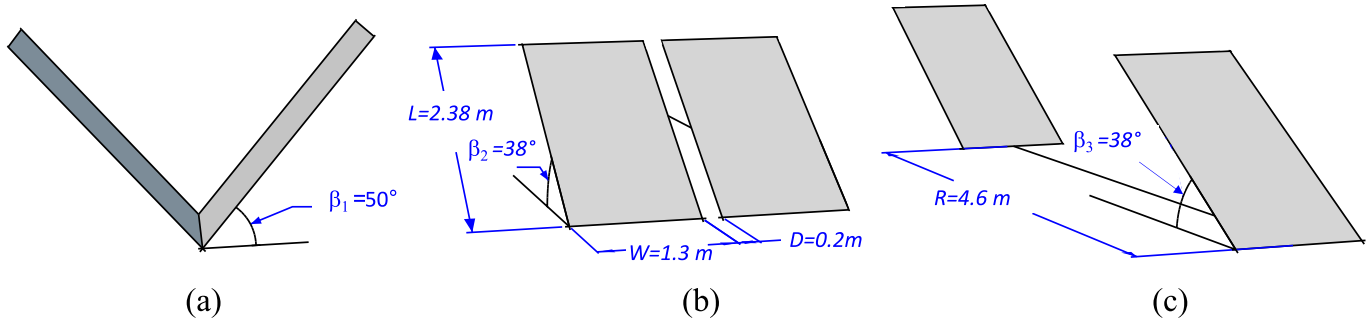

Fig. 5. Schematic representation of the PV module arrangements considered for the comparative analysis: (a) V-configuration, (b) side-by-side configuration, and (c) row-row configuration.

often referred to as the row-to-row pitch [53]. This spacing is designed to prevent mutual shading between rows of panels:

$$GCR = \frac{\text{Total area occupied by PV modules}}{\text{Total ground land area}} = \frac{L}{R} \quad (7)$$

The row-to-row pitch is calculated as follows [53]:

$$R = L \cdot [sin\beta \cdot tan(23.45 + \varphi) + cos\beta] \quad (8)$$

Where:

- L is the length of the PV module [m],
- β is the tilt angle of the PV module, and
- φ is the latitude of the selected location.

The definition of GCR provides a standardized metric for comparing land-use efficiency across different configurations, and emphasised how effectively the array length utilizes the available ground area. This analysis assesses both the annual solar irradiance captured and the land-use efficiency for the V-shaped configuration compared to conventional setups.

3. Results and discussion

Simulations were performed on a workstation equipped with an Intel i9 processor, 128 GB of RAM, and running the latest version of the Ubuntu operating system. The time required to complete a full annual analysis of the V-shaped bifacial photovoltaic system is less than one minute per simulation. This performance metric underscores the model's suitability for both detailed studies and large-scale sensitivity analyses.

3.1. Energy results

To determine the optimal orientation for the two V-shaped panels positioned facing each other, five configurations were simulated by adjusting the azimuth angle of Panel 1. These configurations (*Case a, b, c, d, e*) represent a range of orientations to evaluate the system's performance under different solar exposure scenarios (see Fig. 1).

- *Case a*: Panel 1 faces east and Panel 2 faces west (azimuths 90° and 270°).
- *Case b*: Panel 1 faces southeast and Panel 2 faces northwest (azimuths 135° and 315°).
- *Case c*: Panel 1 faces south and Panel 2 faces north (azimuths 180° and 0°).
- *Case d*: Panel 1 faces southwest and Panel 2 faces northeast (azimuths 225° and 45°).
- *Case e*: Panel 1 faces west and Panel 2 faces east (azimuths 270° and 90°), equivalent to *Case a*.

Table 3 summarizes the annual solar irradiation collected by the panels in each configuration, highlighting the contributions from the front and rear surfaces of both panels (Front 1, Back 1, Front 2, and Back 2). The results indicate that *Case a* and *Case e* yield the highest annual solar irradiation collection, approximately 10,721.4 kWh/year. This confirm that east-west orientation maximizes energy capture under the climatic conditions of Palermo, Italy.

Further analysis (see Fig. 6) highlights how energy output varies across configurations. *Case a* and *Case e* achieve the highest energy production of 2089.3 kWh per panel pair, emphasizing the system's efficiency in capturing solar energy. These two configurations outperform the others by approximately 8 % due to the optimal alignment of panels to maximize exposure during the morning and afternoon solar peaks. *Cases b* and *Cases d* also demonstrate good performance, with energy outputs 3 % and 5 % higher than the baseline, respectively. However, *Cases c* produces the lowest energy output, reflecting the suboptimal south-north orientation for this specific V-shaped system and location, which results in increased shading and reduced exposure during critical solar hours. This analysis underscores the importance of selecting an east-west orientation (as in *Cases a* and *Cases e*) to optimize annual energy production in regions with similar climatic conditions to Palermo. The superior performance of these configurations is further enhanced by the dynamic tilt mechanism, which reduces shading and improves irradiance capture on both front and rear surfaces.

From this point onward, all results refer to the configuration corresponding to *Case a*. Figs. 7.a and 7.b illustrate the variation in the ground projection area of the panels as the sun's position changes across seasons, specifically on June 21st (summer solstice) and December 21st (winter solstice).

As detailed in Subsection 2.1, *System Configuration and Bifacial Module Specifications*, the tilt angle of the panels dynamically varies between 50° and 90° based on solar altitude. In June (see Fig. 7.a), the ground projection area (red line) reaches its maximum between approximately 8:00 a.m. and 4:00 p.m., as the panels minimize their tilt (purple line) to align with the high solar altitude (green line). This alignment not only results in a larger and more consistent ground footprint during peak daylight hours but also ensures efficient light capture by both front and rear surfaces of the bifacial modules. The high solar elevation during this period minimizes shading effects and maximizes irradiance capture, making the system highly effective in summer conditions.

Conversely, in December (see Fig. 7.b), the lower solar elevation and steeper panel tilt angles reduce the projection area, which peaks around midday but remains smaller compared to June. The reduced ground projection area reflects the system's adjustment to the lower sun path, which helps maintain optimal irradiance capture despite shorter daylight hours. However, the sharper fluctuations in the projection area during winter indicate that the system must work harder to adapt to the changing solar angles, leading to slightly reduced efficiency compared to summer. This analysis highlights the system's adaptability to seasonal solar altitude variations. In summer, the dynamic tilt mechanism ensures maximum energy capture by expanding the ground projection area during critical solar hours, while in winter, the steeper tilt angles maintain light capture efficiency despite the reduced solar elevation. These results emphasize the versatility of the V-shaped configuration in optimizing solar energy production across different seasons. Additionally, the shading provided by the panels can moderate extreme temperatures, reducing heat stress on crops, and help conserve soil moisture, improving water use efficiency, particularly in arid regions. While experimental data on crop performance are beyond the scope of this study, these effects align with findings in agrivoltaic research, highlighting the system's dual benefits in energy generation and agricultural resilience [23]. Furthermore, the ability to minimize ground coverage in winter aligns well with the goals of preserving land for agricultural activities, showcasing the system's suitability for agrivoltaic applications.

Table 3
Annual solar irradiation collected by the front and rear sides of each panel.

Solar irradiation [kWh/year]	Case **a**	Case **b**	Case **c**	Case **d**	Case **e**
Front 1	3579.1	4357.2	4804.1	4645.3	3897.6
Back 1	1741.1	1397.4	1120.1	1247.0	1503.5
Front 2	3897.6	2899.2	2319.2	2683.5	3579.1
Back 2	1503.5	1562.4	1608.9	1793.5	1741.1
Total by year	**10,721.4**	**10,216.2**	**9852.3**	**10,369.3**	**10,721.4**

Based on the previous analysis of ground projection and tilt dynamics, Fig. 8.a and Fig. 8.b present the POA irradiance received on the front and rear sides of the two modules in the V-shaped PV configuration during the summer and winter solstices. In summer (see Fig. 8.a), the front sides of the panels experience high irradiance levels, reflecting their orientation toward direct sunlight. Panel 1 captures peak irradiance during the early morning hours, as it east-facing orientation aligns with the rising sun. Conversely, Panel 2, facing west, reaches its irradiance peak in the afternoon as the sun sets. This complementary behavior highlights the effectiveness of the V-shaped configuration in capturing solar energy throughout the day, leveraging the diurnal solar path. The rear sides, by contrast, experiewhile receiving lower irradiance levels, benefit from diffuse and reflected light. These minor peaks indicate the system's ability to utilize secondary light sources, enhancing overall efficiency.

In winter (see Fig. 8.b), the total irradiance levels are significantly reduced due to the lower altitude and shorter daylight period. The front and rear sides of both panels exhibit a more balanced distribution of irradiance, reflecting the dominance of diffuse light under these conditions. This balance is particularly beneficial for bifacial modules, as it maximizes the contribution of the rear surfaces, compensating for the reduced direct irradiance on the front sides.

These results emphasize the seasonal adaptability of the V-shaped configuration. In summer, the system's dynamic tilt mechanism ensures optimal exposure for the front sides during peak solar hours, while maintaining sufficient rear-side irradiance through reflected light. In winter, the configuration shifts to exploit diffuse irradiance more evenly across both surfaces, demonstrating its capacity to adapt to varying solar conditions. This dual advantage supports consistent energy production throughout the year, making the V-shaped configuration particularly effective in regions with significant solar variations. Furthermore, the analysis underlines the importance of optimizing the panel orientation and tilt dynamics to maximize the contribution of both direct and diffuse light. By maintaining high irradiance levels on the front sides during summer and balancing distribution in winter, the system achieves a reliable performance across seasons, which is critical for agrivoltaics application requiring the energy production throughout the year.

Fig. 9.a and Fig. 9.b illustrate the distribution of solar irradiance on the front and rear sides of the two bifacial modules in *Case a* for the Palermo location. The annual energy production of the two modules aligns with this irradiance distribution. Specifically, panel 1 generates 739.65 kWh on the front side and 294.49 kWh on the rear side, while Panel 2 produces 800.78 kWh on the front and 254.40 kWh on the rear. These results underscore the dominant role of the front sides in energy generation, accounting for approximately 72 % of the total energy produced by each panel, with the rear sides contributing a notable, though secondary share.

The energy output distribution highlights the influence of orientation and diurnal solar variation. The front side of the west-facing Panel 2 (Front 2) produces slightly more energy than the east-facing Panel 1 (Front 1), particularly during the summer months. This discrepancy is due to the higher solar irradiance captured by Panel 2 during the afternoon, as solar energy availability peaks during central hour of the day. The orientation of Panel 2 allows it to benefit from longer exposure to high-intensity sunlight, as shown in Fig. 9.b. Conversely, for the rear

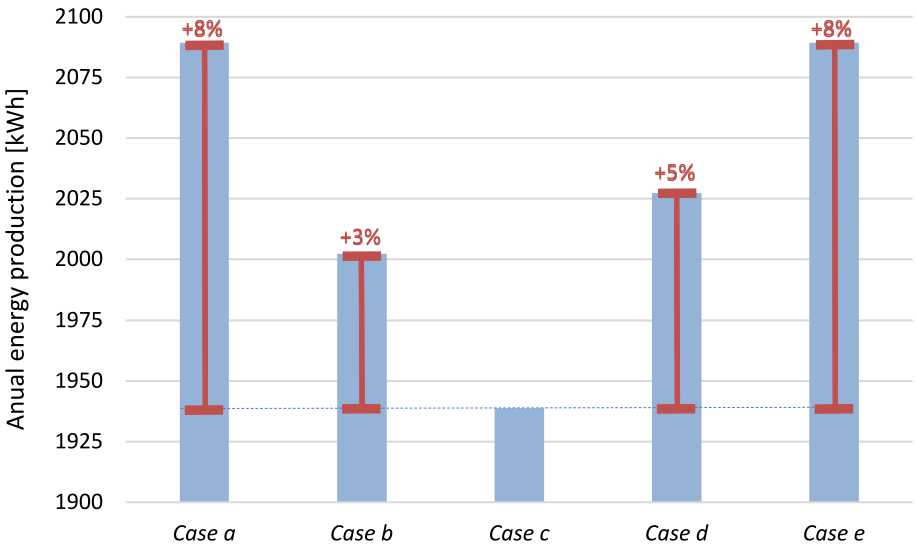

Fig. 6. Annual electricity production obtained by varying the azimuths of the two panels, in Palermo.

side, Panel 1 (Back 1) outperforms Panel 2 (Back 2) in annual energy production. The west-facing orientation of the rear side of Panel 1 enables it to capture greater amounts of reflected and diffuse solar radiation during late afternoon hours, compensating for its lower performance during the early part of the day. This behavior is clearly depicted in Fig. 9.a and Fig. 9.b, where the distribution of irradiance shows higher late-day contributions for the rear side of Panel 1.

These findings demonstrate the significant role of orientation and bifacial technology in optimizing energy capture. While the front sides dominate overall production, the rear sides provide a valuable contribution by capturing reflected and diffuse light, particularly during periods of reduced direct irradiance. The combination of east- and west-facing panels in the V-shaped configuration ensures efficient utilization of solar energy throughout the day, achieving a balance between direct and secondary light sources. This dual-sided contribution is especially advantageous for agrivoltaic systems, where maximizing energy yield with minimal land use is a critical objective.

3.2. Comparative energy analysis with a traditional bPV system without tracking

As detailed in Subsection *2.3, Details of the case study configuration and comparative analysis,* three different arrangements of bifacial PV modules were examined to evaluate differences in solar radiation collection and land-use efficiency. These configurations are defined below (see Fig. 5):

- *Configuration a*: Panels are arranged in a V-shaped configuration, with Panel 1 facing east and Panel 2 facing west. The tilt of the panels varies dynamically between 50° and 90°
- *Configurations b*: Panels are positioned side by side with a fixed tilt equal to the latitude of the installation site (38° for Palermo), ensuring no mutual shading (see Fig. 5.b).
- *Configuration c:* Panels are arranged one behind the other in a row-to-row setup, also with a fixed tilt of 38° (see Fig. 5.c).

For each configuration, the annual solar irradiance collected was evaluated using the custom algorithm developed in this study, with results summarised in Table 4.

The analysis revealed that *Configuration a* collects 5.2 % less annual solar irradiation compared to *Configuration b* and *Configuration c*, achieving a total of 10,721.4 kWh/year compared to 11,312.4 kWh/year. Despite this slight reduction in irradiation, the V-shaped arrangement (*Configuration a*) demonstrates a remarkable advantage in terms of land-use efficiency. Specifically, *Configuration a* requires only 3.98 m^2 of ground area, compared to 5.25 m^2 for *Configuration b* (side-by-side) and 8.38 m^2 for *Configuration c* (row-to-row), translating to a 24 % and 53 % reduction, respectively. This significant land-saving potential underscores the V-shaped configuration's suitability for applications where land availability is constrained, such as agrivoltaics systems. The Ground Coverage Ratio (GRC), a key metric for evaluating spatial efficiency, further highlights these differences:

- ***Configuration a*** (V-shaped): With a GCR of 1.56, this arrangement minimizes land-use efficiency through its compact design and dynamic tilt mechanism.
- ***Configuration b*** (side-by-side): Achieving a GCR of 1.1, this configuration offers moderate land-use optimization. Panels arranged side by side with 0.2 m spacing, effectively balance space efficiency with solar exposure.
- ***Configuration c*** (row-to-row): Featuring a GCR of 0.74, this arrangement is the least efficient in terms of land use. The 4.6 m row-to-row pitch required to prevent shading significantly increases the land area occupied. While this configuration maximizes solar radiation capture, it does so at the cost greater land use.

These findings underscore the trade-offs between land-use efficiency and solar irradiance capture. In conclusion, the choice of configuration depends on the specific priorities of the photovoltaic installation. *Configuration a* offers a compelling solution where land availability is constrained, while *Configuration c* may be more suitable for maximizing energy generation in locations where land use is not a primary concern.

Starting from the preliminary analysis of land-use efficiency and radiation capture, the annual energy production of two PV system layouts was compared. These layouts were designed for a one-hectare vineyard, assuming the installation of one bifacial PV panel row between every two rows of vines. This arrangement aims to balance agricultural productivity with energy generation, maximizing the dual land-use potential of agrivoltaic systems. A schematic representation of the two analysed layouts is provided in Fig. 10:

- *Layout A:* This layout features bifacial PV panels arranged in a V-shape (according to *Configuration a*) and incorporates the previously analysed solar tracking system. The panels dynamically adjust their tilt throughout the day based on the solar altitude to maximize sunlight exposure. The bifacial modules are oriented with one panel

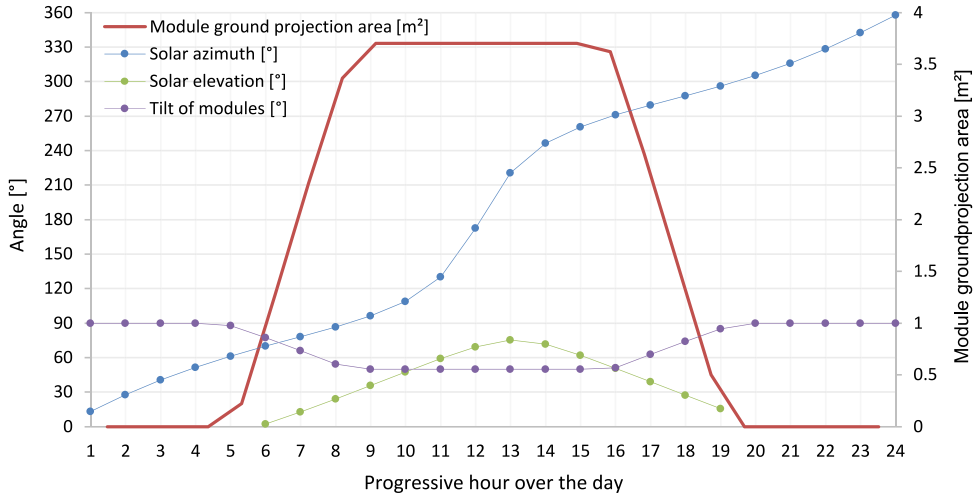

(a)

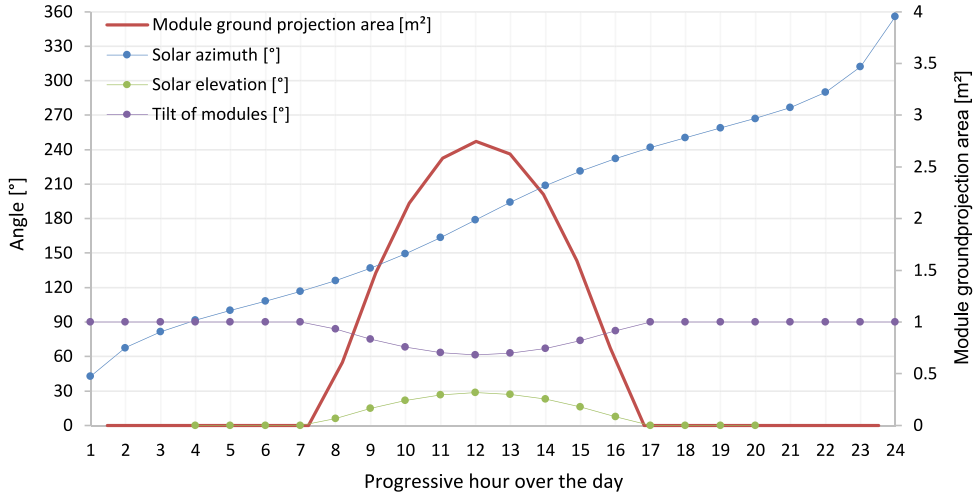

(b)

Key Definitions:

- *Solar azimuth angle:* The angle of the sun's rays in the horizontal plane, measured from true south (northern hemisphere) or true north (southern hemisphere) [54].
- *Solar elevation angle:* The angle formed between the horizontal plane and the sun's incoming rays [54].
- *Tilt of module:* The angle between the plane of a solar panel and the horizontal ground [55].

Fig. 7. Azimuth and solar elevation angles, module tilt angles, along with the projected area of the module surface on the ground on the summer and winter solstices days: (a) June 21st and (b) December 21st [54,55].

facing east and the other west, with the apex of the V aligned along the north-south axis. The distance between rows of vines was assumed to be 2.5 m, with a minimum spacing of 1.25 m between the vine rows and the edges of the PV panels. Considering the maximum V-opening and the dimensions of the selected panels, the total spacing between two rows of vines, with a PV row positioned in between, is 5.5 m, while pairs of panels within the same PV row are spaced 2 m apart. Under these assumptions, the field can accommodate 660 modules per hectare, resulting in a total peak power of 438.9 kW_p and a GCR of 0.2.

- *Layout B:* This layout uses the same bifacial PV modules as Layout A but positions them with a fixed tilt of 38° facing south, arranged in a row-to-row configuration (according to *Configuration c*). In Layout B, the same bifacial PV modules selected for the V-shape are used but are installed with a fixed tilt of 38° facing south. The distance between rows of vines, with a PV row positioned in between, is reduced to 3.8 m compared to Layout A, while the spacing between modules within the same PV row is fixed at 4.6 m to prevent mutual shading effects [56]. This arrangement allows the installation of 315 modules per hectare, resulting in a total peak power of 209.5 kW_p and a GCR of 0.097.

This comparison highlights the distinct characteristics of each layout. Layout A prioritizes land-use efficiency and higher power capacity, while Layout B offers a more compact arrangement with reduced spacing requirements but a lower peak power output. The trade-offs between land use, module spacing and energy production underscore the importance of tailoring PV system configurations to the specific

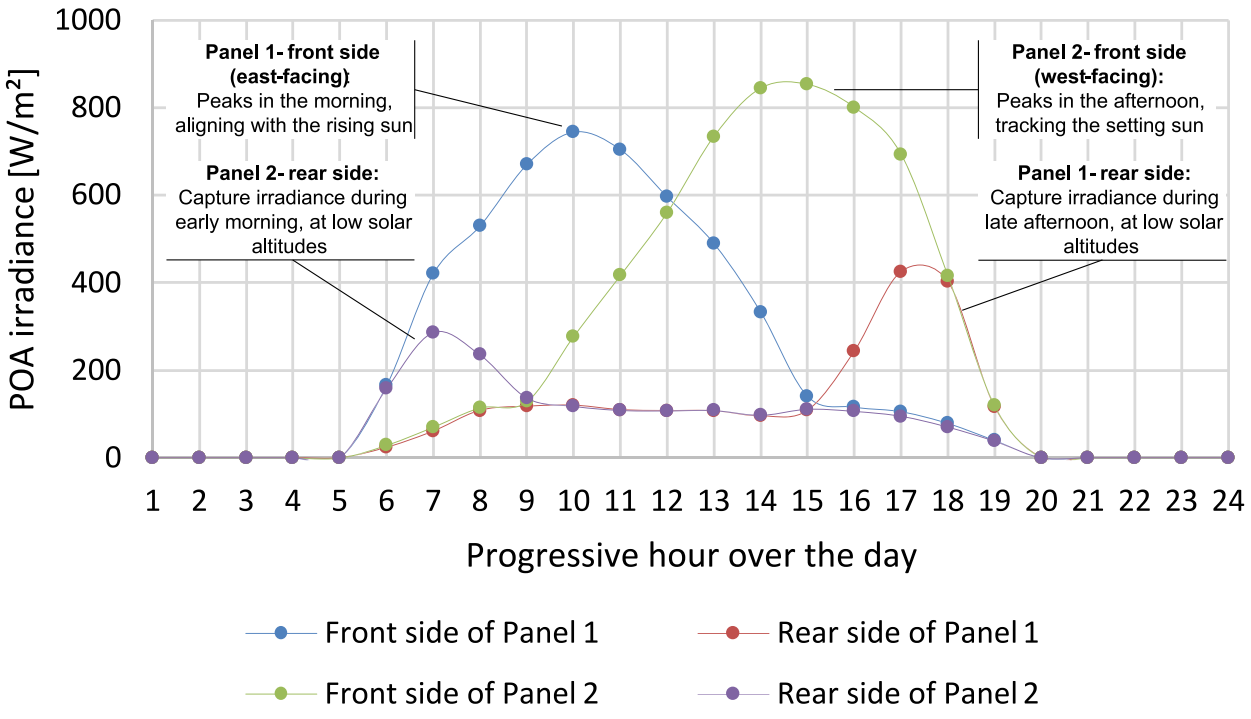

(a)

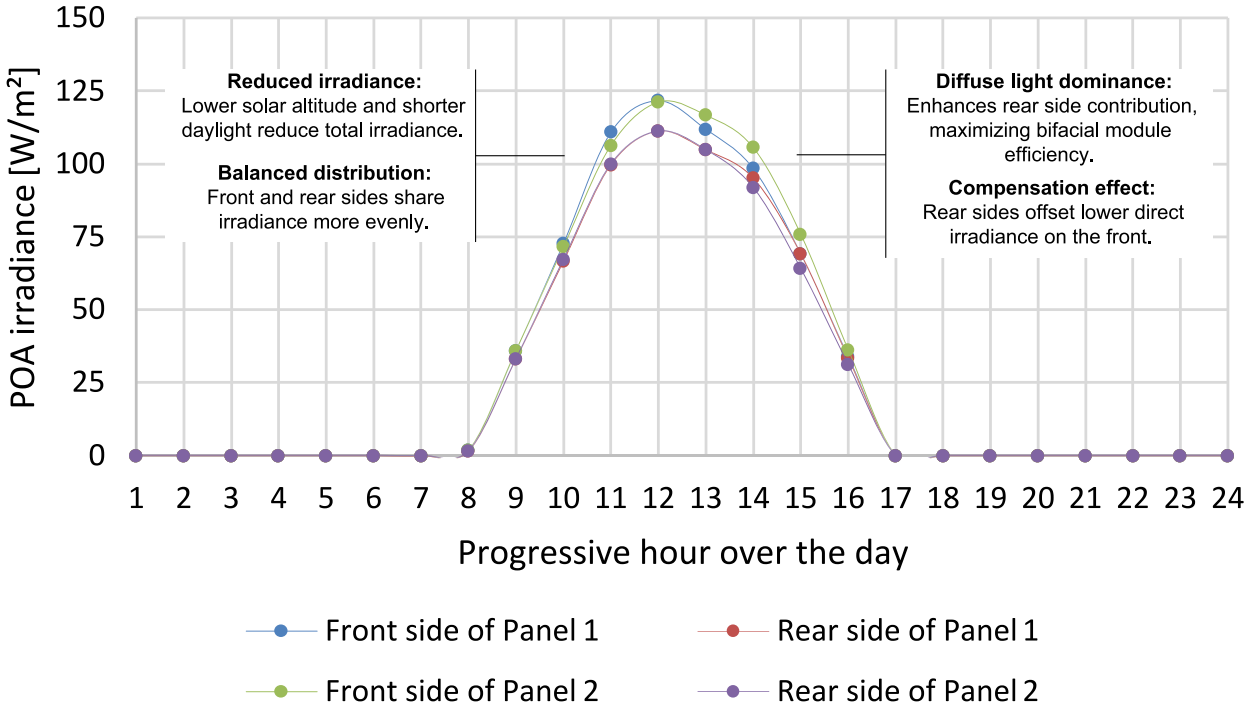

(b)

Fig. 8. Solar irradiance incident on the front and rear surfaces of the bifacial PV modules on the summer and winter solstices days: (a) June 21st and (b) December 21st.

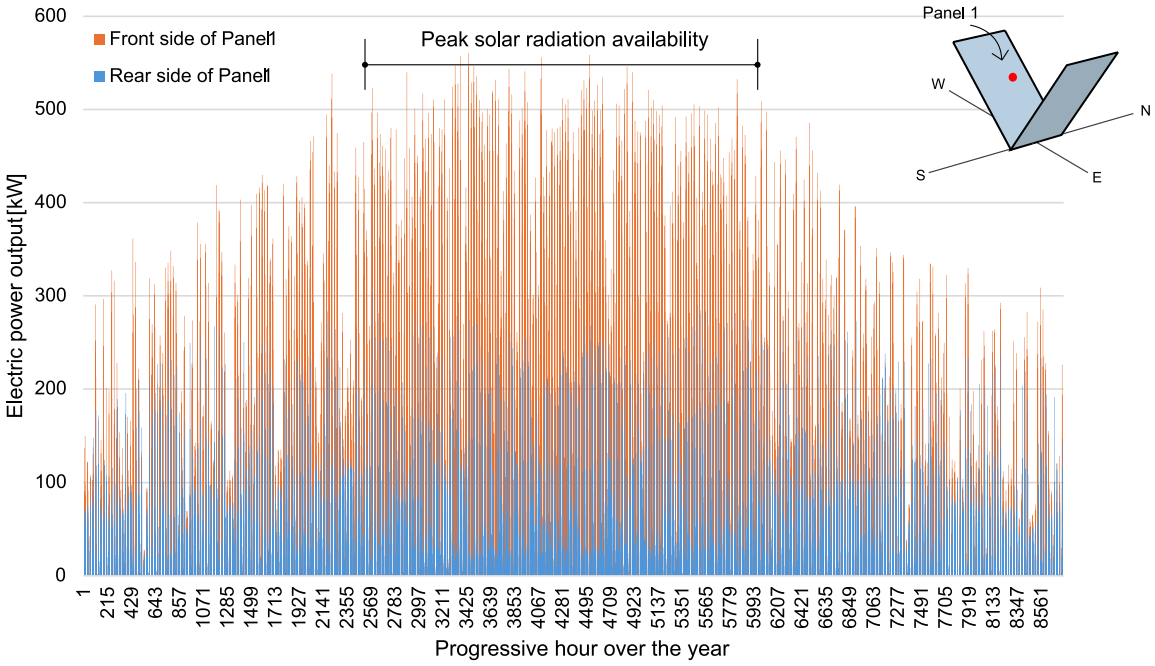

Electric power output	Count	Mean	Standard deviation	Min	25th Percentile	Median	75th Percentile	Max	Total
Front 1	8760	85.8	135.2	0	0	0	118.0	566.4	739.7
Back 1	8760	34.2	54.1	0	0	0	50.8	305.5	294.5

(a)

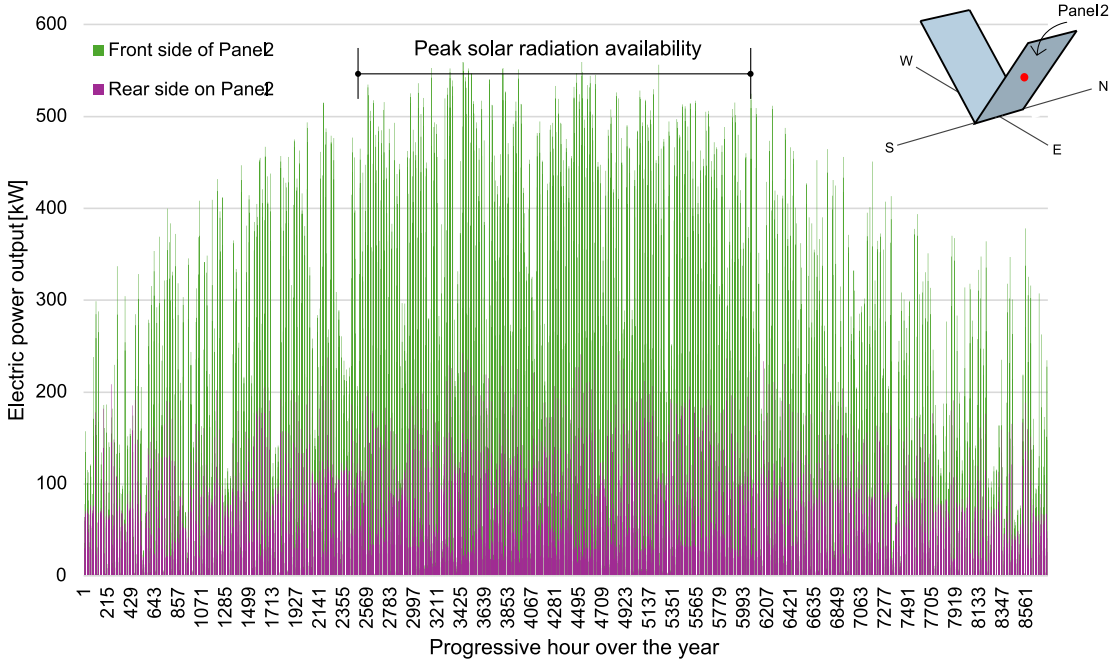

Electric power output	Count	Mean	Standard deviation	Min	25th Percentile	Median	75th Percentile	Max	Total
Front 2	8760	92.9	145.1	0	0	0	140.2	564.7	800.8
Back 2	8760	29.5	43.1	0	0	0	47.9	242.4	254.4

(b)

Fig. 9. Hourly electric power output of the bifacial PV modules in Palermo: (a) Panel 1 facing east and (b) Panel 2 facing west.

Table 4
Annual solar irradiation collected by two bifacial PV panels under different configurations.

Solar irradiation [kWh/year]	***Configuration a***	***Configurations b*** or ***c***
Front 1	3579.1	4695.4
Back 1	1741.1	960.8
Front 2	3897.6	4695.4
Back 2	1503.5	960.8
Total by year	**10,721.4**	**11,312.4**

requirements of agrivoltaic applications.

This detailed analysis underscores the fundamental differences in spatial layouts and module densities between the two configurations, along with their respective impacts on energy production and land-use efficiency. Layout A, with its dynamic V-shaped tracking system, achieves a higher installed capacity and demonstrates superior land-use efficiency, despite necessitating wider spacing between vine rows. Conversely, Layout B, with fixed south-facing panels, offers a simpler and more compact design but results in lower installed capacity and reduced land-use efficiency. Using the algorithm developed in this study, the annual energy output for the two layouts was quantified for Palermo's climatic conditions. Layout A was found to produce 551.6 MWh per year, corresponding to 1256.7 equivalent hours, while Layout B generated 286.5 MWh per year, with 1367.7 equivalent hours.

These results clearly demonstrate the dual benefits of Layout A: enhanced energy production and superior land-use efficiency. By dynamically adjusting panel tilt, the V-shaped configuration minimizes shading, maximizes irradiance capture, and accommodates a higher number of modules per hectare. In contrast, Layout B sacrifices energy yield and spatial efficiency due to the fixed tilt and increased row spacing required to prevent mutual shading.

These findings are particularly relevant for agrivoltaic applications, where balancing energy production with agricultural productivity is crucial. Both configurations comply with Italian agrivoltaic regulations, maintaining low ground coverage ratios. However, Layout A's ability to combine high energy output with efficient land use positions it as the more suitable option for scenarios where land availability is limited or agricultural activities need to be preserved.

The innovative use of dynamic tilt adjustments in the V-shaped bifacial PV system provides clear advantages in terms of energy production and land-use efficiency. However, this comes at a cost: the dynamic system involves higher initial investments due to the need for tracking mechanisms and more frequent maintenance compared to fixed-tilt configurations. Despite these added complexities, the benefits of dynamic tilt adjustments outweigh the costs in scenarios where maximizing energy yield and optimizing land use are critical, such as in agrivoltaic applications. By enabling higher energy productivity with a compact design, the system proves particularly advantageous for applications in land-constrained areas, such as vineyards or other high-value agricultural regions. Future research should conduct detailed cost-benefit analyses to quantify these trade-offs further, ensuring economic feasibility across diverse implementation contexts.

4. Conclusions

This study explores an innovative agrivoltaic system utilizing bifacial photovoltaic modules arranged in a V-shaped configuration with a single-axis tracking mechanism. A custom Python-based simulation model, developed with the PVlib library, was employed to evaluate the system's performance by incorporating mutual shading, multiple reflections, and dynamic tilt adjustments. The system's performance was analysed under the climatic conditions of Palermo, southern Italy.

The key findings demonstrate that the proposed V-shaped configuration achieves an annual energy output of 2089.3 kWh per pair of panels, capturing 5.2 % less solar radiation compared to traditional side-by-side setups. However, it significantly enhances land-use efficiency, reducing land occupancy by 24 % (3.98 m^2 vs. 5.25 m^2 for conventional setups). When scaled to a one-hectare vineyard, the system achieved an annual energy production of 551.6 MWh, nearly double the 286.5 MWh generated by a fixed-tilt row-to-row configuration. This underscores the system's superior integration of energy productivity and land-use optimization, making it particularly advantageous for agrivoltaics applications. A pilot project at the University of Palermo, in collaboration with the company Horizonfirm, is being implemented to verify the performance of the model developed and to identify possible new improvements to the system under consideration.

The Python-based model developed in this study emerges as a versatile and adaptable tool for analysing complex agrivoltaic configurations. Its flexibility, including the ability to work with any Typical Meteorological Year (TMY) dataset, allows for applications across various climatic conditions, alternative PV designs, and diverse agricultural contexts, providing a framework for detailed and realistic simulations. This adaptability ensures the model's applicability to a

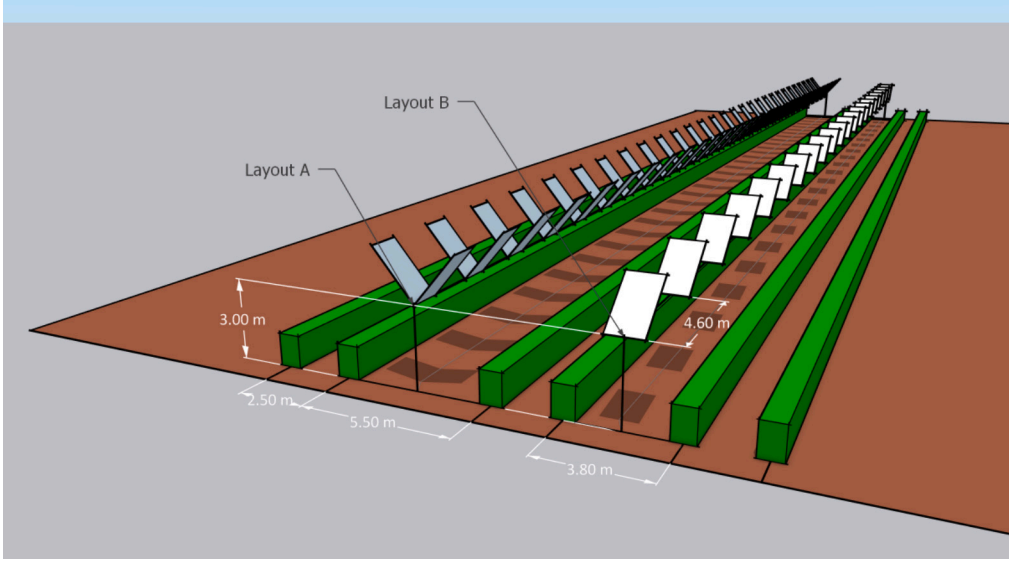

Fig. 10. Schematic representation of the two plant layouts compared: Layout A and Layout B.

wide range of geographic locations and climatic scenarios. However, challenges remain when adapting the model to configurations with highly irregular geometries or unconventional system designs. Additionally, while the model is computationally efficient for site-specific analyses, scaling up to simulate large systems or conducting extensive sensitivity analyses may demand significant computational resources. Addressing these aspects in future work would enhance the model's scalability and practical utility.

This adaptability opens pathways for further exploration, including:

- Extending the model to incorporate economic analyses, such as cost-benefit evaluations and payback period assessments, to determine the financial feasibility of the proposed system.
- Performing sensitivity analyses on parameters like albedo, bifaciality, and module temperature to improve the accuracy and robustness of the simulation results.
- Applying the model to different crop types and geographic regions to assess its versatility and broader environmental implications.

In addition to these future directions, further research could benefit from collaborative efforts among engineers, agronomists, and climatologists to optimize both energy production and agricultural productivity. Such collaboration could lead to holistic solutions that balance renewable energy generation with sustainable agriculture, addressing the dual challenges of food and energy security. Moreover, assessing the system's impact on the surrounding environment – such as changes in soil quality, water retention, and microclimatic conditions – would provide a more comprehensive understanding of its sustainability and long-term viability. Exploring the adaptability of the V-shaped configuration in extreme climatic conditions, such as arid regions or high-latitude areas, could further expand its applicability and address unique environmental challenges. Additionally, the implementation of pilot projects in real-world contexts would be useful to validate model predictions and refine both system design and simulation approaches. These field tests could also offer insight into practical deployment and operational efficiency under diverse agrivoltaics scenarios.

While the proposed V-shaped bifacial PV system aligns with Italian agrivoltaic regulations, its applicability could be further enhanced by considering international regulatory frameworks. Future research should explore how the system can meet diverse requirements globally, including those related to land-use policies, energy efficiency, and agricultural sustainability in regions such as the European Union, the United States, and Asia. Such an analysis would provide valuable insights into the scalability and adaptability of the system in different geographic and regulatory contexts.

To enhance the system's overall performance, future research should also investigate its integration with emerging technologies, such as advanced energy storage, smart grids, and AI-based optimization tools. These innovations could significantly improve operational intelligence and energy management, making the system more adaptable and efficient in dynamic energy markets.

Finally, incorporating sustainability metrics such as life cycle cost analysis and water savings into future studies would provide more comprehensive evaluation of the system's environmental and economic impact. These analyses are particularly relevant for regions facing water scarcity or high agricultural demands, where optimizing resource use is critical. By examining these aspects, future research can contribute to a broader understanding of the V-shaped bifacial PV system's role in advancing sustainable energy and land-use practices.

Overall, the findings emphasize that the V-shaped bifacial module configuration offers a promising solution for agrivoltaic systems. This innovative approach not only enhances energy capture efficiency but also optimizes land use while minimizing its impact on agricultural activities. The system demonstrates clear advantages in annual energy production compared to traditional configurations while adhering to regulatory constraints and maintaining low ground coverage.

It is important to highlight that the unique design of the proposed panel system poses challenges that could not be addressed with conventional tools and commercially available software. Existing solutions lacked the flexibility to simulate the specific geometric and operational characteristics of the V-shaped bifacial PV configuration. This study successfully addressed these limitations by leveraging the exceptional adaptability of the Python programming environment. Python's open and modular architecture facilitated the development of customized algorithms tailored to the complexities of the system. Additionally, the robustness of the PVlib library played a pivotal role in providing accurate solar position calculations, irradiance modelling, and performance simulations. Together, these tools created a comprehensive platform capable of solving the intricate issues posed by innovative agrivoltaic design.

Future research should focus on conducting in-depth evaluations of the system's economic sustainability. This entails detailed cost-benefit analyses that consider installation, maintenance, and operational costs against energy yields and potential agricultural advantages. Additionally, research on the scalability of this approach in different regions and its integration with emerging energy and agricultural technologies will be critical for supporting the global transition toward sustainable energy and land use practices.

Nomenclature

Symbols

I_{MPP}	Maximum Power Current [A]
I_{SC}	Short Circuit Current [A]
L	Length of the PV module [m]
L'	Total length of the PV array [m]
P_{max}	Peak Power Watts [W_p]
R	Minimum distance between successive rows [m]
V_{MPP}	Maximum Power Voltage [V]
V_{OC}	Open Circuit Voltage [V]
W	Width of the PV module [m]

Greek letters

β	Tilt angle of the PV module, and [°]
φ	Latitude of the selected location [°]

Acronyms

AOI	Angle of Incidence
APV	Agrivoltaic
COP	Conference of the Parties
DHI	Diffuse horizontal irradiance
DNI	Direct Normal Irradiance
GCR	Grand coverage ratio
GHG	Greenhouse gas
GHI	Global horizontal irradiance
IAM	Incidence Angle Modifier
IRENA	International Renewable Energy Agency
LCOE	Levelized Cost of Electricity
MPPT	Maximum Power Point Tracking
NOCT	Nominal Operating Cell Temperature
POA	Plane-of-array
PV	Photovoltaic
TMY	Typical Meteorological Year

CRediT authorship contribution statement

Stefania Guarino: Writing – original draft, Software, Methodology, Investigation, Formal analysis, Conceptualization. **Alessandro Buscemi:** Investigation, Conceptualization. **Christian Chiaruzzi:**

Investigation, Conceptualization. **Valerio Lo Brano:** Supervision, Software, Methodology, Investigation, Formal analysis, Conceptualization.

Declaration of competing interest

The authors declare the following financial interests/personal relationships which may be considered as potential competing interests: Christian Chiaruzzi has patent System of photovoltaic solar panels for installation in a field for agricultural or pastoral use, and energy production method using this system issued to Horizonfirm S.R.L., Viale Francesco Scaduto 2/D, I-90144 Palermo (IT). If there are other authors, they declare that they have no known competing financial interests or personal relationships that could have appeared to influence the work reported in this paper.

Acknowledgments

The authors extend their heartfelt thanks to HorizonFirm S.r.l. and Eng. Christian Chiaruzzi for their invaluable support, which was essential for conducting this study.

Appendix A. Supplementary data

Supplementary data to this article can be found online at https://doi.org/10.1016/j.apenergy.2025.125785.

Data availability

No data was used for the research described in the article.

References

[1] (IPCC) IP on CC. Mitigation Pathways Compatible with 1.5°C in the Context of Sustainable Development. Glob. Warm. 1.5°C. Cambridge University Press; 2022. p. 93–174. https://doi.org/10.1017/9781009157940.004.
[2] COP28, IRENA, and GRA. Tripling renewable power and doubling energy efficiency by 2030: Crucial steps towards 1.5°C. Abu Dhabi: International Renewable Energy Agency; 2023.
[3] United Nations Framework Convention on Climate Change (UNFCCC). UN Climate Change Conference Baku - November 2024. https://unfccc.int/cop29; 2024.
[4] Ember.. Share of electricity generated by fossil fuels – Ember and energy institute. Stat Rev World Energy 2024.
[5] Ritchie H. Rosado P. Our World Data: Electricity Mix; 2020.
[6] IRENA. Renewable capacity statistics 2024, International Renewable Energy Agency. Abu Dhabi. 2024.
[7] IRENA. Renewable power generation costs in 2023. Abu Dhabi 2024.
[8] IRENA. World energy transitions outlook 2024: 1.5°C pathway. Abu Dhabi 2024.
[9] Gomez-Casanovas N, Mwebaze P, Khanna M, Branham B, Time A, DeLucia EH, et al. Knowns, uncertainties, and challenges in agrivoltaics to sustainably intensify energy and food production. Cell Reports Phys Sci 2023;4(8):101518.
[10] Gasparatos A, Doll CNH, Esteban M, Ahmed A, Olang TA. Renewable energy and biodiversity: implications for transitioning to a green economy. Renew Sust Energ Rev 2017;70:161–84. https://doi.org/10.1016/j.rser.2016.08.030.
[11] Hernandez RR, Easter SB, Murphy-Mariscal ML, Maestre FT, Tavassoli M, Allen EB, et al. Environmental impacts of utility-scale solar energy. Renew Sust Energ Rev 2014;29:766–79. https://doi.org/10.1016/j.rser.2013.08.041.
[12] Ali B, Hedayati-Dezfooli M, Gamil A. Sustainability assessment of alternative energy power generation pathways through the development of impact indicators for water, land, GHG emissions, and cost. Renew Sust Energ Rev 2023;171:113030. https://doi.org/10.1016/j.rser.2022.113030.
[13] Jiang J, Gao X, Lv Q, Li Z, Li P. Observed impacts of utility-scale photovoltaic plant on local air temperature and energy partitioning in the barren areas. Renew Energy 2021;174:157–69. https://doi.org/10.1016/j.renene.2021.03.148.
[14] Nemet GF. Net radiative forcing from widespread deployment of photovoltaics. Environ Sci & Technol 2009;43:2173–8.
[15] Coakley JA. Reflectance and albedo, surface. Encycl Atmos Sci 2003:1914–23.
[16] Santbergen R, van Zolingen RJC. The absorption factor of crystalline silicon PV cells: A numerical and experimental study. Sol Energy Mater Sol Cells 2008;92:432–44.
[17] Wu W, Yue S, Zhou X, Guo M, Wang J, Ren L, et al. Observational study on the impact of large-scale photovoltaic development in deserts on local air temperature and humidity. Sustainability 2020;12:3403.
[18] Barron-Gafford GA, Minor RL, Allen NA, Cronin AD, Brooks AE, Pavao-Zuckerman MA. The photovoltaic Heat Island effect: larger solar power plants increase local temperatures. Sci Rep 2016;6:35070. https://doi.org/10.1038/srep35070.
[19] Dupraz C, Talbot G, Marrou H, Wery J, Roux S, Liagre F, et al. To mix or not to mix: Evidences for the unexpected high productivity of new complex agrivoltaic and agroforestry systems. In: Proc. 5th world Congr. Conserv. Agric. Resilient food Syst. A Chang. world; 2011.
[20] Jerez S, Tobin I, Vautard R, Montávez JP, López-Romero JM, Thais F, et al. The impact of climate change on photovoltaic power generation in Europe. Nat Commun 2015;6:10014. https://doi.org/10.1038/ncomms10014.
[21] Dinesh H, Pearce JM. The potential of agrivoltaic systems. Renew Sust Energ Rev 2016;54:299–308. https://doi.org/10.1016/j.rser.2015.10.024.
[22] Torrente CJ, Reca J, López-Luque R, Martínez J, Casares FJ. Simulation model to analyze the spatial distribution of solar radiation in agrivoltaic Mediterranean greenhouses and its effect on crop water needs. Appl Energy 2024;353:122050. https://doi.org/10.1016/j.apenergy.2023.122050.
[23] Al Mamun MA, Dargusch P, Wadley D, Zulkarnain NA, Aziz AA. A review of research on agrivoltaic systems. Renew Sust Energ Rev 2022;161:112351. https://doi.org/10.1016/j.rser.2022.112351.
[24] Yadav D, Singh N, Bhadoria VS, Vita V, Fotis G, Tsampasis EG, et al. Analysis of the factors influencing the performance of single- and multi-diode PV Solar modules. IEEE Access 2023;11:95507–25. https://doi.org/10.1109/ACCESS.2023.3306473.
[25] Abdullah BUD, Lata S, Jaiswal SP, Bhadoria VS, Fotis G, Santas A, et al. A hybrid artificial ecosystem optimizer and incremental-conductance maximum-power-point-tracking-controlled grid-connected photovoltaic system. Energies 2023;16. https://doi.org/10.3390/en16145384.
[26] Williams HJ, Wang Y, Yuan B, Wang H, Zhang KM. Rethinking agrivoltaic incentive programs: A science-based approach to encourage practical design solutions. Appl Energy 2025;377:124272. https://doi.org/10.1016/j.apenergy.2024.124272.
[27] Wimalasekera R. Effect of light intensity on photosynthesis. Photosynth Product Environ Stress 2019:65–73.
[28] Mouhib E, Fernández-Solas Á, Pérez-Higueras PJ, Fernández-Ocaña AM, Micheli L, Almonacid F, et al. Enhancing land use: integrating bifacial PV and olive trees in agrivoltaic systems. Appl Energy 2024;359:122660.
[29] Zainali S, Ma Lu S, Stridh B, Avelin A, Amaducci S, Colauzzi M, et al. Direct and diffuse shading factors modelling for the most representative agrivoltaic system layouts. Appl Energy 2023;339:120981. https://doi.org/10.1016/j.apenergy.2023.120981.
[30] Sojib Ahmed M, Rezwan Khan M, Haque A, Ryyan Khan M. Agrivoltaics analysis in a techno-economic framework: understanding why agrivoltaics on rice will always be profitable. Appl Energy 2022;323:119560. https://doi.org/10.1016/j.apenergy.2022.119560.
[31] Toledo C, Scognamiglio A. Agrivoltaic systems design and assessment: A critical review, and a descriptive model towards a sustainable landscape vision (three-dimensional agrivoltaic patterns). Sustain 2021:13. https://doi.org/10.3390/su13126871.
[32] Fernández-Solas Á, Fernández-Ocaña AM, Almonacid F, Fernández EF. Potential of agrivoltaics systems into olive groves in the Mediterranean region. Appl Energy 2023;352:121988. https://doi.org/10.1016/j.apenergy.2023.121988.
[33] Willockx B, Reher T, Lavaert C, Herteleer B, Van de Poel B, Cappelle J. Design and evaluation of an agrivoltaic system for a pear orchard. Appl Energy 2024;353:122166. https://doi.org/10.1016/j.apenergy.2023.122166.
[34] Gorjian S, Bousi E, Özdemir ÖE, Trommsdorff M, Kumar NM, Anand A, et al. Progress and challenges of crop production and electricity generation in agrivoltaic systems using semi-transparent photovoltaic technology. Renew Sust Energ Rev 2022;158:112126. https://doi.org/10.1016/j.rser.2022.112126.
[35] Padilla J, Toledo C, Abad J. Enovoltaics: symbiotic integration of photovoltaics in vineyards. Front Energy Res 2022:10. https://doi.org/10.3389/fenrg.2022.1007383.
[36] Malu PR, Sharma US, Pearce JM. Agrivoltaic potential on grape farms in India. Sustain Energy Technol Assessments 2017;23:104–10. https://doi.org/10.1016/j.seta.2017.08.004.
[37] Agostini A, Colauzzi M, Amaducci S. Innovative agrivoltaic systems to produce sustainable energy: an economic and environmental assessment. Appl Energy 2021;281:116102. https://doi.org/10.1016/j.apenergy.2020.116102.
[38] Amaducci S, Yin X, Colauzzi M. Agrivoltaic systems to optimise land use for electric energy production. Appl Energy 2018;220:545–61. https://doi.org/10.1016/j.apenergy.2018.03.081.
[39] Hussain SN, Ghosh A. Evaluating tracking bifacial solar PV based agrivoltaics system across the UK. Sol Energy 2024;284:113102. https://doi.org/10.1016/j.solener.2024.113102.
[40] Willockx B, Lavaert C, Cappelle J. Performance evaluation of vertical bifacial and single-axis tracked agrivoltaic systems on arable land. Renew Energy 2023;217:119181. https://doi.org/10.1016/j.renene.2023.119181.
[41] F. Holmgren W, W. Hansen C, A. Mikofski M.. Pvlib Python: a Python package for modeling Solar energy systems. J Open Source Softw 2018;3:884. https://doi.org/10.21105/joss.00884.
[42] Anderson KS, Hansen CW, Holmgren WF, Jensen AR, Mikofski MA, Driesse A. Pvlib python: 2023 project update. J Open Source Softw 2023;8:5994.
[43] Jensen AR, Anderson KS, Holmgren WF, Mikofski MA, Hansen CW, Boeman LJ, et al. Pvlib iotools—open-source Python functions for seamless access to solar irradiance data. Sol Energy 2023;266:112092. https://doi.org/10.1016/j.solener.2023.112092.
[44] Chiaruzzi Christian; Costantino Agostino. System of photovoltaic solar panels for installation in a field for agricultural or pastoral use, and energy production method using this system. WO 2024/009219 A1. 2025.

[45] Ministero della Transizione Ecologica. Decreto del 15 settembre 2022 – Linee guida in materia di agrivoltaico. Gazzetta Ufficiale della Repubblica Italiana, Serie Generale n 2022;224.
[46] Holmgren WF, Hansen CW, Mikofski MA. Pvlib python: A python package for modeling solar energy systems. J Open Source Softw 2018;3:884.
[47] Sandia National Laboratories PPMC (PVPMC). Plane of Array (POA) Irradiance. https://pvpmc.sandia.gov/modeling-guide/1-weather-design-inputs/plane-of-array-poa-irradiance/; 2025.
[48] Faiman D. Assessing the outdoor operating temperature of photovoltaic modules. Prog Photovolt Res Appl 2008;16:307–15.
[49] pvlib python. pvlib.irradiance.get_total_irradiance. https://pvlib-python.readthedocs.io/en/v0.9.0/generated/pvlib.irradiance.get_total_irradiance.html#pvlib.irradiance.get_total_irradiance; 2025.
[50] pvlib python. pvlib.iam.physical. https://pvlib-python.readthedocs.io/en/v0.9.0/generated/pvlib.iam.physical.html#id5; 2025.
[51] pvlib python. pvlib.temperature.faiman. https://pvlib-python.readthedocs.io/en/v0.9.0/generated/pvlib.temperature.faiman.html; 2025.
[52] Trina Solar. https://www.trinasolar.com/it/product/VERTEX-DEG21C.20; 2025 (accessed October 27, 2023).
[53] Doubleday K, Choi B, Maksimovic D, Deline C, Olalla C. Recovery of inter-row shading losses using differential power-processing submodule DC–DC converters. Sol Energy 2016;135:512–7.
[54] Kalogirou SA. 3.01 - Solar Thermal Systems: Components and Applications—Introduction☆. In: Letcher TM, editor. Compr. Renew. Energy. Second Ed. Second Edi. Oxford: Elsevier; 2022. p. 1–25. https://doi.org/10.1016/B978-0-12-819727-1.00001-7.
[55] Kalogirou SA. Chapter 9 - photovoltaic systems. In: Kalogirou SA, editor. Sol. Energy Eng. Second Ed. Second ed. Boston: Academic Press; 2014. p. 481–540. https://doi.org/10.1016/B978-0-12-397270-5.00009-1.
[56] Kalogirou S. Solar energy engineering: processes and systems: second edition. Sol Energy Eng Process Syst. Second Ed 2009.